LONG-TERM EVOLUTIONARY LINKS BETWEEN HIGH-MAGNETIC-FIELD RADIO PULSARS AND DIM ISOLATED NEUTRON STARS

by
ŞEYDA ÖZCAN

Submitted to the Graduate School of Engineering and Natural Sciences
in partial fulfilment of
the requirements for the degree of Master of Science

Sabancı University
Dec 2020

LONG-TERM EVOLUTIONARY LINKS BETWEEN HIGH-MAGNETIC-FIELD RADIO PULSARS AND DIM ISOLATED NEUTRON STARS

Approved by:

Date of Approval: Dec 24, 2020

ABSTRACT

LONG-TERM EVOLUTIONARY LINKS BETWEEN HIGH-MAGNETIC-FIELD RADIO PULSARS AND DIM ISOLATED NEUTRON STARS

ŞEYDA ÖZCAN

Physics, Master of Science Thesis, DEC 2020

Thesis Supervisor: Prof.Dr. ÜNAL ERTAN

The long-term evolution of the neutron stars with fallback disks depends on their initial conditions, namely the initial period of the star, P_0, the mass of the disk, M_d, and the magnetic dipole field at the poles of the star, B_0. There are three basic evolutionary paths characterized by the sequences of the rotational phases (weak propeller or strong propeller) that can be followed by a neutron star over its long-term evolution. For a chosen set of initial conditions, a model source can evolve following one of these basic paths. In this work, first, we have investigated how these initial conditions affect the evolutionary paths of the sources. Later, we have described the evolutionary paths and the current phases of the isolated neutron star populations based on the results obtained earlier in the fallback disk model. These populations are anomalous X-ray pulsars (AXPs), soft gamma repeaters (SGRs), rotating radio transients (RRATs), central compact objects (CCOs), dim isolated neutron stars (XDINs) and high-B radio pulsars (HBRPs). The radio pulsar PSR J0726–2612, discovered recently, has the rotational and X-ray properties similar to those of XDINs and HBRPs. The characteristic age of the source is about an order of magnitude smaller than those of XDINs. In the fallback disk model, XDINs are not expected to show pulsed radio emission. Nevertheless, this radio pulsar apparently seems to evolve towards the XDIN properties. In the magnetar model, the non-detection of radio pulses from XDINs are assumed to be due to narrow beaming of their radio emission. It was proposed that PSR J0726–2612 could be the first XDIN with pulsed radio emission observable due to convenient viewing geometry. In the second part of this work, through numerical simulations, we have analyzed the allowed initial conditions and the evolutionary avenues that can produce the properties of the source consistently with its radio pulsar behaviour in the fallback disk model. Our results indicate that the evolutionary path followed by this source is similar to those of HBRPs. The B_0 estimated for PSR J0726–2612 places the source above the pulsar death line. The rotational properties and X-ray luminosity of the source are obtained simultaneously at an age of $t \sim 5 \times 10^4$ yr. Our model results indicate that PSR J0726–2612 will reach the ages of XDINs (several 10^5 yr) as a normal radio pulsar, rather than the XDIN properties.

ÖZET

YÜKSEK MANYETİK ALANLI RADYO PULSARLARI VE SÖNÜK İZOLE NÖTRON YILDIZLARI ARASINDAKİ BAĞIN UZUN DÖNEM EVRİMİNİN İNCELENMESİ

ŞEYDA ÖZCAN

Fizik, Yüksek Lisans Tezi, ARALIK 2020

Tez Danışmanı: Prof.Dr. ÜNAL ERTAN

Nötron yıldızlarının kalıntı diskleri ile uzun dönem evrimi, başlangıç koşullarına, yani yıldızın başlangıç periyoduna (P_0), diskin kütlesine (M_d) ve yıldızın kutuplarındaki manyetik dipol alanı şiddetine (B_0) bağlıdır. Uzun dönem evrimi boyunca bir nötron yıldızının takip edebileceği dönme fazlarını (zeyıf pervane ve güçlü pervane) karakterize eden üç temel evrimsel yol vardır. Seçilen başlangıç koşulları için, bir model kaynak bu temel yollardan birini izleyerek evrimleşebilir. Bu çalışmada ilk olarak, bu başlangıç koşullarının kaynakların evrimsel yollarını nasıl etkilediğini araştırdık. Daha sonra, kalıntı diski modelinde daha önce elde edilmiş sonuçlara dayanarak izole nötron yıldızı popülasyonlarının evrimsel yollarını ve mevcut fazlarını tanımladık. Bu popülasyonlar, anormal X-ışını pulsarları (AXP'ler), gama ışını tekrarlayıcıları (SGR'ler), geçici dönen radyo kaynakları (RRAT'ler), merkezi yoğun cisimler (CCO'lar), sönük izole kaynaklar (XDIN'ler) ve yüksek manyetik alanlı radyo pulsarlarıdır (HBRP'ler). Yakın zamanda keşfedilen radyo pulsar PSR J0726–2612, XDIN'ler ve HBRP'lerinkine benzer dönme özelliklerine ve X ışını parlaklığına sahiptir. Kaynağın karakteristik yaşı yaklaşık olarak XDIN'lerinkinden daha küçüktür. Kalıntı disk modelinde, XDIN'lerin düzenli radyo emisyonu göstermesi beklenmez. Ancak, bu kaynak XDIN özelliklerine doğru gelişiyor gibi görünüyor. Magnetar modelinde, XDIN'lerden radyo sinyali tespit edilmemesinin, bu kaynakların dar radyo ışımasından kaynaklandığı varsayılır. PSR J0726–2612'nin, uygun görüntüleme geometrisi nedeniyle gözlemlenebilen düzenli radyo emisyonlu ilk XDIN olabileceği önerildi. Bu çalışmanın ikinci bölümünde, nümerik simülasyonlar aracılığıyla, bu kaynağın dönme ve X-ışını özelliklerini üretmeye izin veren başlangıç koşullarını, radyo pulsar davranışıyla tutarlı bir şekilde üretebilen evrimsel yolları analiz ettik. Sonuçlarımız, bu kaynağın evrimini açıklayan yolun, HBRP'lerinkine benzer olduğunu göstermektedir. PSR J0726–2612 için tahmin edilen B_0, kaynağı pulsar ölüm çizgisinin üstüne yerleştirir. Kaynağın dönme özellikleri ve X ışını parlaklığını eş zamanlı olarak $t \sim 5 \times 10^4$ y yaşında elde etmekteyiz. Model sonuçlarımız, PSR J0726–2612'nin XDIN kaynaklarının yaşlarına, bir XDIN olarak değil, normal bir radyo pulsarı özellikleriyle (birkaç $\sim 10^5$ y) ulaşacağını göstermektedir.

ACKNOWLEDGEMENTS

I would like to thank my advisor Prof. Ünal Ertan for his patience and encouragement in my studies. His guidance not only helped me with my thesis and academic studies but also in my private life as well. He was always acquaintanced with the difficulties that I was facing and he has always been understanding towards me. Without his support, I would not be able to achieve my degree and could not have enjoyed my studies as much as I did during my master.

I would like to thank my fellow friends in the field. Their support and friendship motivated me in my studies both in courses and in our research.

I am also thankful to all my friends who believed in me and encouraged my studies in every possible way for them. Especially, I thank Merjem Hazic for taking care of me and my daughter during the last two month. Also, I thank my friends Meryem, Fikriye, Kübranur, Elvan, Mervenur and more for always being there for me. Finally, I am thankful to my family for their support.

I dedicate this study to my daughter, Meryem.

TABLE OF CONTENTS

LIST OF ABBREVIATIONS

AXP   Anomalous X-ray Pulsars

SGR   Soft Gamma Repeater

XDIN   Dim Isolated Neutron Star

HBRP   High Magnetic Field Radio Pulsar

CCO   Central Compact Object

RRAT   Rotation Radio Transient

LMXB   Low Mass X-ray Binary

HMXB   High Mass X-ray Binary

XRB   X-ray Binary

MSP   Millisecond Pulsar

1.   INTRODUCTION

The idea of neutron star came immediatly after the discovery of neutron by Chadwick (1932). Baade & Zwicky (1934) proposed that supernove could be the events forming neutron stars from normal stars. It was proposed that protons and electrons are likely to come together to form neutrons at high densities (Sterne, 1933). Sterne calculated the mass density required to become a neutron rich matter one year after the discovery of neutron. In 1936, George Gamow argued that neutron-rich cores could exist at the centers of massive stars connecting the neutron physics to astrophysical objects which supports the idea proposed by Baade & Zwicky (1934). Later, Oppenheimer & Volkoff (1939) studied the structure and estimated a mass of $\sim \frac{3}{4} M_\odot$ for a neutron star. Tolman (1939) also obtained similar results through analytical calculations. Cameron (1959) estimated an upper limit of $\sim 2 M_\odot$ to the mass of a neutron star.

Despite these theoretical estimates, the existence of neutron stars was questioned until the discovery of the first radio pulsar (PSR 1919+21) by Jocelyn Bell in 1967. It was regularly pulsating with period $P = 1.377$ s (Hewish et al., 1968) indicating that PSR 1919+21 should be a neutron star. Because, these very regular pulses can only be produced by rotation, and only neutron stars can rotate with such short periods. The first X-ray pulsar, Sco X-1 was discovered in 1962 before the discovery of PSR 1919+21, but could not be identified as a neutron star immediately. Later, many X-ray pulsars were discovered in 1970s. Today, it is commonly accepted that X-ray pulsars are neutron stars powered by mass accretion from their companion stars, as proposed earlier by Shklovsky (1967) for Sco X-1.

Neutron stars are the most compact objects that we can directly observe in the universe. They are formed by supernova events at the end of the evolutions of massive stars. Depending on the mass of the progenitor star, a supernova could produce a neutron star or a black hole. If neutron degeneracy pressure can support the core against gravity, the core becomes a neutron star. Otherwise, collapse goes on leading to formation of a black hole. The minimum critical mass for blackhole formation is estimated to be $\sim 3 M_\odot$ (Cameron, 1959). The estimated masses and

radii for most of the known neutron stars are $\sim 1.4 M_\odot$ and ~ 10 km respectively, which corresponds to an enormous average density of $\sim 10^{15}$ g cm^{-3}. Because of the angular momentum and magnetic flux conservation during the collapse, the newly born star can rotate very fast with periods as short as several milliseconds, and have very strong magnetic dipole fields with strength $B \sim 10^{11} - 10^{13}$ G on the surface of the star. Neutron stars are not only the most compact but also the fastest rotating objects of the observable universe. They provide an excellent laboratory to study physics in these extreme conditions.

Mass accretion onto a neutron star converts rest-mass energy into radiation more efficiently than in fusion reactions (see e.g Frank et al., 2002). Neutron stars in binary systems are bright X-ray sources powered by mass accretion from the companion, which are called X-ray binaries (XRBs). Depending on the mass of the companion star, M_c, XRBs are classified into two groups: high-mass X-ray binaries (HMXBs) and low-mass X-ray binaries (LMXBs). Among XRBs, those with $M_c >$ several $M_\odot$ are classified as HMXBs. In most of these systems, the neutron star accretes matter from the wind of the companion (van den Heuvel & Heise, 1972; Bondi & Hoyle, 1944). Their rotational periods are in the range of $60 - 850$ s (White, 2002) and $B \sim 10^{12}$ G (Bhalerao et al., 2015). XRBs with $M_c \lesssim M_\odot$ are called LMXBs (Lewin et al., 1997). For most LMXBs, the mass flow from the companion is estimated to occur through Roche-lope overflow, forming a geometrically thin accretion disk around the neutron star. Rotational periods of neutron stars in these systems are mostly in the milliseconds range. Discovery of these millisecond pulsars (MSPs) in LMXBs, starting from 1998 (Wijnands & van der Klis, 1998), confirmed the idea that MSPs are the neutron stars that were spun up by the accretion torques in LMXBs (Alpar et al., 1982; Radhakrishnan & Srinivasan, 1982). Their surface magnetic dipole fields are weak ($B \sim 10^8 - 10^9$ G; Burderi & D'Amico, 1997), which is likely to be due to field decay associated with accretion processes during the long-term evolution (Srinivasan et al., 1990; Konar & Bhattacharya, 1997). Geometrically thin discs could also form in HMXBs through Roche-lobe overflow for some sufficiently close binaries (Bachetti et al., 2014). One example for this type of HMXBs could be Cen X-3 observed with UHURU (Giacconi et al., 1971). In the case of Roche-lobe overflow, the matter flows into the Roche-lobe of the neutron star with a large angular momentum. This prevents the transferred material from directly falling onto the neutron star and leads to formation of a thin accretion disc (e.g. Frank et al., 2002). The inner disk is cut at a radius depending on the dipole field strength of the neutron star, while the outer disk is cut by the strong tidal forces of the companion. The disk matter moves with Keplerian speeds at all radii. By means of viscous torques operating along the disk, angular

momentum is transferred outwards while the matter flows inwards.

Since the discovery of first radio pulsar in 1967, more than 2500 radio pulsars have been detected. With developing observational techniques used onboard the new satellites like ROSAT, ASCA, RXTE and EINSTEIN, several young or mature isolated (single) neutron star populations were discovered with different characteristic properties in the last ~ 30 years (Pavlov et al., 2001; Abdo et al., 2013). These neutron star systems are anomalous X-ray pulsars (AXPs), soft gamma repeaters (SGRs), rotating radio transients (RRATs), central compact objects (CCOs), dim isolated neutron stars (XDINs, also called "the magnificent seven") and high-B radio pulsars (HBRPs). Beside their distinguishing radiative and rotational properties, these systems also show some similarities. Considering that all of them are isolated neutron stars, what could be the physical reasons causing the emergence of all these different populations?

AXPs were discovered in the soft X-ray band (< 10 keV) with luminosities $L_x \sim 10^{33}$–10^{36} erg s^{-1}, much higher than the rotational powers, $\dot{E}_{rot} = I\Omega\dot{\Omega}$, for most of these systems, where I is the moment of inertia, Ω and $\dot{\Omega}$ are the angular frequency of the neutron star and its time derivative respectively. These high X-ray luminosities of AXPs cannot be explained by the intrinsic cooling of the star either. SGRs were discovered in the soft γ-ray band with energetic short bursts. The periods of SGRs and AXPs are clustered between 2 and 12 s, with $\dot{P} \sim 10^{-12} - 10^{-10}$ s s^{-1}. Assuming that the magnetic dipole torque is the only external torque acting on the star, the field strength at the poles is inferred to be $B_d = 6.4 \times 10^{19}\sqrt{P\dot{P}} > 10^{14}$ G for most of these systems. Hereafter, we use "B_d" to denote this dipole field strength deduced with the assumption that the source is rotating in vacuum. We will use "B_0" to denote the actual magnetic dipole field at the pole of the star which is not equal to B_d in the presence of other external torques. In addition to normal gamma bursts, three SGRs also showed giant bursts with $L \gtrsim 10^{44}$ erg s^{-1}. The soft gamma bursts that were observed later also from AXPs (Kaspi et al., 2003) indicated that AXPs and SGRs are likely to belong to the same population. Most of the AXP/SGRs do not show radio pulses. Among the 23 known AXP/SGRs, the radio pulsations observed from only four sources have properties quite different from the normal radio pulses. Their proximity to the galactic plane and supernova associations of some of them indicate that they are young neutron star systems (see e.g. Mereghetti, 2013, for a review of AXP/SGRs).

Central compact objects (CCOs) are also young neutron stars found at the centers of supernova remnants (Gotthelf et al., 2013). For 10 confirmed CCOs, $L_x \sim 10^{32} - 10^{33}$ erg s^{-1}, and no radio or optical counterparts have been detected.

The P and $\dot{P}$ values that were measured only for three sources are in the ranges of $P \sim 0.1 - 0.4$ s and $\dot{P} \sim 10^{-18} - 10^{-17}$ s s^{-1}, which give $B_d \sim 10^{10}$ G, lowest among the isolated neutron star populations. Their L_x values are greater than the rotational powers, like most of the other young neutron star populations.

Rotating radio transients (RRATs) were detected in the last two decades (McLaughlin et al., 2006). They show sporadic radio bursts lasting several milliseconds with recurrence time-scales ranging from minutes to hours. RRATs are estimated to have the highest birth rate among the isolated neutron star populations (Popov et al., 2006). This means that the observational properties of RRATs are crucial to understand the possible evolutionary connections between the neutron star populations. The P and $\dot{P}$ values have been measured for 34 sources out of 105 confirmed RRATs (for details, see Keane et al., 2011). Their periods are distributed over a large range from 0.13 s to 7.7 s. Only one of these sources (PSR J1819-1458) was detected in X-rays (Reynolds et al., 2006).

The first X-ray dim isolated neutron star (XDIN) was discovered in 1990s (Walter et al., 1996). There are seven known XDINs (also known as the "magnificient seven"). They are characterized by their purely thermal blackbody radiation in X-ray band and large X-ray to optical flux ratios. Simple statistical analysis imply that XDINs also have a high birth rate close to that of RRATs (Popov et al., 2006). Their periods are clustered in the $\sim 3 - 17$ s range similar to AXP/SGR periods. These periods together with $\dot{P} \sim 10^{-14} - 10^{-13}$ s s^{-1} give $B_d \sim 10^{13} - 10^{14}$ G. XDINs have L_x in the $\sim 10^{31} - 10^{32}$ erg s^{-1} range. XDINs are observable with these low L_x, since all of them are located within about 500 pc. No pulsed radio emission was detected from these sources.

HBRPs are the radio pulsars with $P \sim 0.1 - 7.7$ s and $\dot{P} \sim 10^{-14} - 10^{-12}$ s s^{-1}, which give $B_d \sim$ a few $10^{13} - 10^{14}$ G (from the dipole-torque formula), in the B_d range of AXP/SGRs. The spin-down powers of these sources are higher than their L_x values, like normal radio pulsars. SGR like bursts were also detected from one HBRP, namely PSR J1846-0258 (Gavriil, 2008).

In the magnetar model (Duncan & Thompson, 1992; Thompson & Duncan, 1995), all these neutron star populations are assumed to be rotating in vacuum and slowing down by the magnetic dipole torques, $\Gamma_B \approx 2\mu^2\Omega^3/3c^3$ where μ is the magnetic dipole moment, and c is the speed of light. With this assumption, magnetic dipole field strength at the poles is estimated to be $B_d \simeq 6.4 \times 10^{19}\sqrt{P\dot{P}}$ G which gives $B_d \gtrsim 10^{14}$ G for most of AXP/SGRs. In this model, the decay of these strong fields was proposed to be the source of their persistent L_x. The soft gamma bursts of AXP/SGRs requires magnetar fields, but these fields do not have to be in the

dipole components. Small-scale quadropole fields could also power these bursts (see the discussion in Chapter 4). With these inferred strong dipole fields, most of these populations, including XDINs and RRATs, are located above the pulsar death line. Nevertheless, these sources do not show radio pulses. In this model, the lack of radio pulses is assumed to be due to narrow beaming of radio emission and the viewing geometry.

Part of the supernova matter could fall back and form disks around the neutron stars (Colgate, 1971; Chevalier, 1989; Michel & Dessler, 1981). In the presence of a fallback disk, the disk torque dominates the magnetic dipole torque in most cases. The B_d value deduced from the dipole torque formula from the observed P and $\dot{P}$ overestimates the actual field strength, B_0, by one to three orders of magnitude. The disk torque should be estimated through numerical calculations in different phases of the long-term evolution. Fallback disks were proposed to explain the X-ray luminosities and the period clustering of AXPs (Chatterjee et al., 2000). Alpar (2001) proposed that if the fallback disk properties are included in the initial conditions, in addition to the dipole moment and the initial period, the properties of other neutron star populations could also be explained. In this model, the accretion from the fallback disk to the magnetic poles of the star explains the observed pulsed X-ray emission of these sources, while the period clustering of AXPs is explained as a natural outcome of the long-term interaction between the disk and the star. The fallback disk model was developed later including the effects of X-ray irradiation of the disk including the contribution of the cooling luminosity, and the inactivation of disk at low temperatures (see e.g. Ertan et al., 2014). In a series of works, supporting the idea proposed by Alpar et al. (2011), it was shown that the properties of AXP/SGRs (Ertan et al., 2009; Benli & Ertan, 2016), CCOs (Benli & Ertan, 2018b), XDINs (Ertan et al., 2014), HBRPs (Benli & Ertan, 2017, 2018a) and RRATs (Gençali & Ertan, 2018, 2020) can be accounted for with very similar basic disk parameters (see Chapter 2).

This model is described in Chapter 2, with a discussion about the effects of the initial conditions on the evolution of the sources. In Chapter 3, we give the details of the application of the model to the debated source PSR J0726-2612. We discuss the results obtained earlier in the fallback disk model, together with our results in the present work, and summarize our conclusions in Chapter 4.

2.   LONG-TERM EVOLUTION OF NEUTRON STARS WITH

FALLBACK DISK

2.1 THE MODEL

In this chapter, we summarize the long-term evolution model for neutron stars with fallback disks, which was applied earlier to different isolated neutron star populations. In this model, we solve the disk diffusion equation

$$(2.1) \qquad \frac{\partial \Sigma}{\partial t} = \frac{3}{r} \frac{\partial}{\partial r} \left(r^{1/2} \frac{\partial}{\partial r} \left(\nu \Sigma r^{1/2} \right) \right)$$

(see e.g. Frank et al., 2002) where Σ is surface density of the disk, r is radial distance from the center of the star, $\nu = \alpha c_s h$ is the kinematic viscosity, α is the kinematic viscosity parameter, c_s is the speed of sound, and h is the half thickness of the disk (Shakura & Sunyaev, 1973).

There is a critical temperature, T_{p}, below which the disk enters viscously inactive phase. This occurs starting from the cold outermost disk. The radius, at which the local temperature of the disk currently equals T_{p}, is the dynamical outer radius, r_{out}, of the active disk. In the long-term evolution, r_{out} moves inwards with decreasing L_x, that is, $r_{\mathrm{out}} = r(T = T_{\mathrm{p}})$. There are two main mechanisms heating up the disk: the viscous dissipation in the disk, and the X-ray irradiation by the emission from the neutron star. The effective temperature of the disk is given by

$$(2.2) \qquad T_{\mathrm{eff}} \simeq [(D + F_{\mathrm{irr}})/\sigma]^{1/4}$$

where σ is Stefan-Boltzman constant, D is the rate of viscous dissipation per unit disk area. The irradiation flux can be written as $F_{\mathrm{irr}} = 1.2\, CL_{\mathrm{x}}/\pi r^2$, where C is the irradiation efficiency parameter which includes disk geometry and the albedo of the disk surface, L_{x} is the total X-ray luminosity of the neutron star (Fukue, 1992).

Both accretion and the intrinsic cooling of the neutron stars contribute to L_x. To find the cooling luminosity, L_{cool}, at a given age, we use the theoretical cooling curve estimated for neutron stars with conventional dipole fields (Page et al., 2006). The accretion from the inner disk radius, r_{in}, to the surface of the neutron star produces the accretion luminosity

$$(2.3) \qquad L_{acc} = \frac{GM\dot{M}_*}{R}$$

where G is gravitational constant, M is mass of the neutron star, and $\dot{M}_*$ is the mass accretion rate to the surface of the neutron star, and R is the radius of the neutron star. The total luminosity of the disk can be written as

$$(2.4) \qquad L_D = \frac{GM\dot{M}_{in}}{2\,r_{in}}$$

where $\dot{M}_{in}$ is the mass-inflow rate of the disk. Most of L_D is emitted from the innermost disk regions. When there is mass flow onto the star, $L_D = (\,R/2r_{in})L_{acc}$. For all the isolated neutron star populations $r_{in} >> R$, and the inner disk, radiating mostly in the optical and IR bands, does not contribute to L_x. The total X-ray luminosity of the star can be written as $L_x = L_{acc} + L_{cool}$, while L_{acc} dominate L_{cool} in most cases.

When the accretion is allowed in the spin-down (weak propeller, WP) phase, we calculate the disk torque acting on the star by integrating the magnetic torques from the Alfvén radius, $r_A = [\mu^4/(GM\dot{M}_{in}^2)]^{1/7}$ to the co-rotation radius, $r_{co} = (GM/\Omega_*^2)^{1/3}$ where μ is the magnetic dipole moment of the star, Ω_* is the angular frequency of the neutron star. At the co-rotation radius, Kepler speed of the disk matter is equal to the speed of the closed field lines rotating with the neutron star. The result of this integration can be written as

$$(2.5) \qquad N_D = \frac{1}{2}\dot{M}_{in}(GMr_A)^{1/2}[1 - (r_A/r_{co})^3]$$

(Ertan & Erkut, 2008). Another contribution to the spin-down torque comes from the magnetic dipole radiation, $N_{dip} = -2\mu^2\Omega_*^3/3c^3$, which is mostly negligible compared to N_D. The spin-up torque associated with the accretion onto the star $N_{acc} = \dot{M}_*(GMr_{in})^{1/2}$ where $r_{in} = r_{co}$ in the WP phase. The total torque, $N_{TOT} = N_D + N_{acc} + N_{dip}$, becomes

$$(2.6) \quad N_{TOT} = \frac{1}{2}\dot{M}_{in}(GMr_A)^{1/2}[1 - (r_A/r_{co})^3] + (G\,M\,r_{co})^{1/2}\dot{M}_* - 2\mu^2\Omega_*^3/3c^3 \;.$$

Below a certain $\dot{M}_{\mathrm{in}}$, r_{A} exceeds the light cylinder radius, $r_{\mathrm{LC}} = c/\Omega_*$, where c is the speed of light. In this case, we replace r_{A} with r_{LC} in Eq. 2.6. Since there is not a well known critical $\dot{M}_{\mathrm{in}}$ for the transition from the WP to the strong propeller (SP) phase, we assume that this transition takes place when $r_{\mathrm{A}} = r_{\mathrm{LC}}$. Because of the sharp decrease in $\dot{M}_{\mathrm{in}}$ during this transition, the exact value of the critical $\dot{M}_{\mathrm{in}}$ does not affect our results significantly. In the SP phase, only the spin-down torques act on the star, since $\dot{M}_* = 0$ in this phase.

In the model, main disk parameters (α, C, and T_{p}) are expected to be similar for the fallback disks of different neutron star systems assuming that they have similar chemical compositions. In the earlier applications of this model to AXP/SGRs, CCOs, HBRPs, XDINs, and RRATs, reasonable results were obtained with $\alpha = 0.045$, $T_{\mathrm{p}} \sim (50-150)$ K, and $C = (1-7) \times 10^{-4}$ (see e.g. Benli & Ertan, 2016). The initial conditions P_0, B_0, and M_{d} of the neutron star could be different for different sources, leading to diverse long-term evolutionary paths.

2.2 EFFECT OF INITIAL CONDITIONS ON THE LONG-TERM

EVOLUTION

There are three basic long-term evolutionary paths of the neutron stars evolving with fallback disks. A given source follow one of these paths depending on its initial conditions P_0, B_0, and M_d.

Path (1): WP + SP. These sources start their evolution in the WP phase. In a long-term WP phase, their rotation is slowed down by the disk torques to periods longer than a few seconds depending mainly on their B_0 values. Due to these long periods, except for very restricted set of initial conditions, these sources find themselves below the pulsar death line after the WP/SP transition. **Path (2): Always in the SP phase.** These sources never enter into the WP phase, evolve as HBRPs in the early phases, and approach to the normal radio pulsar properties at late phases of evolution. Eventually, their radio pulses are switched off above a critical period. **Path (3): SP + WP + SP.** These sources start their evolution in the SP phase identified as HBRPs. Unlike in path 2, evolution starts with an increasing $\dot{P}$. This goes on until $\dot{P}$ reaches its maximum and enters the WP phase. In the WP phase of paths (1) and (3), the sources could be identified as persistent or transient AXP/SGRs. After a long-lasting WP phase, the sources eventually enter back into the SP phase when the accretion terminates. Like in path (1), the
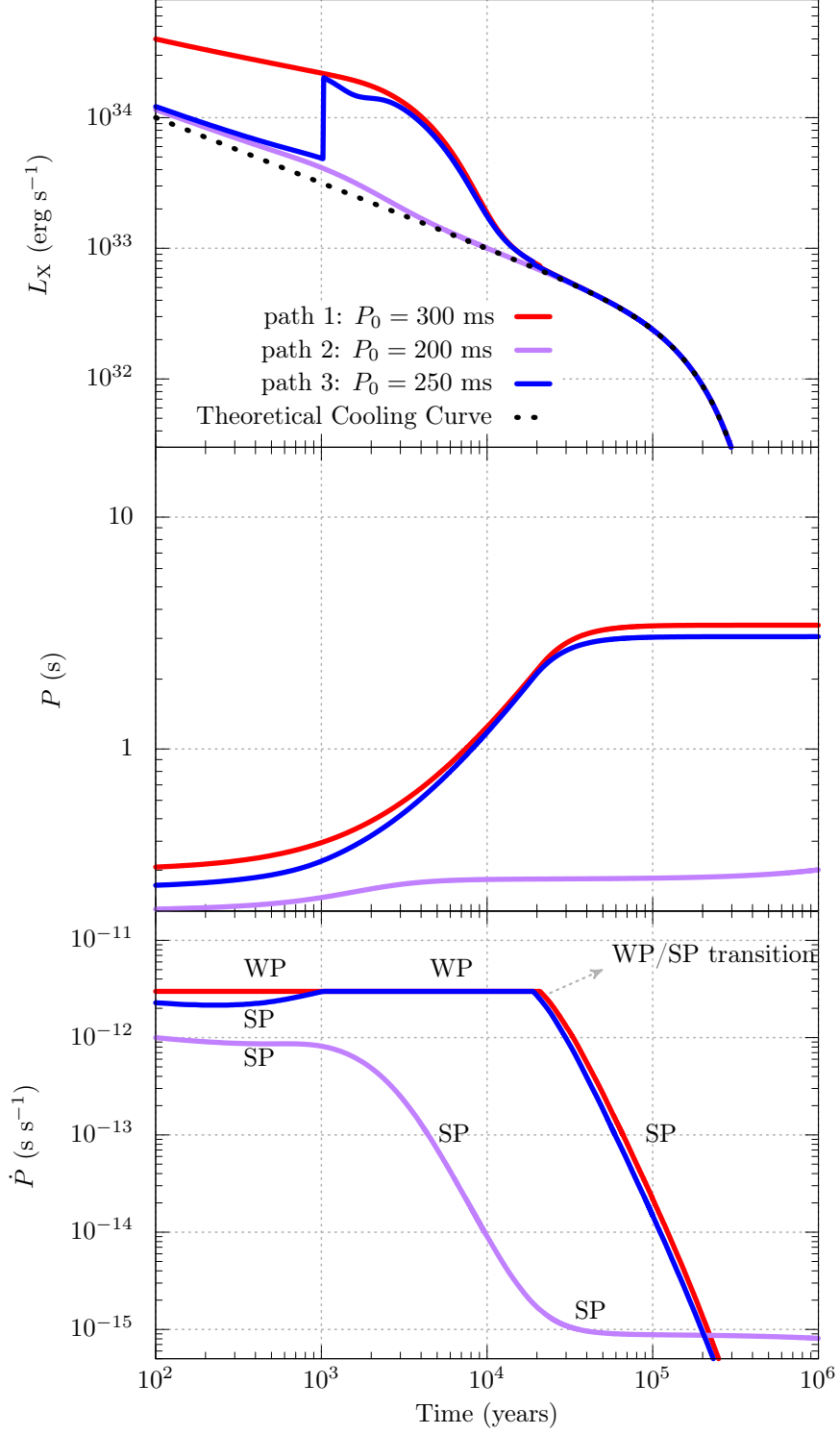
Figure 2.1 These illustrative model curves are obtained with different values of initial period, P_0. For all these models, $B_0 = 10^{12}$ G, and $M_d \simeq 3.16 \times 10^{-6} M_\odot$. All the model curves seen in Figs. 1, 2, and 3 are obtained with the same set of main disk parameters ($\alpha = 0.045$, $C = 10^{-4}$, and $T_p = 100$ K). The rotational phases (WP or SP) are also indicated on the model curves.

long periods reached at the end of the WP phase place the neutron star below the pulsar death line after the WP/SP transition. During the WP phases, pulsed radio emission is not allowed either because of mass flow onto the neutron star. The sources with $B_0 \sim$ a few $10^{11} - 10^{12}$ G acquire the XDIN properties in the final SP phases of the path (1) and (2), while the sources with weaker fields could show RRAT behaviour (Gençali & Ertan, 2020).

Below, with some illustrative model curves, we will show how each of the initial conditions, namely P_0, B_0, and M_d, affect the evolutionary paths of the stars.

The Initial Period, P_0. The model curves given in Fig. 2.1 show the effect of P_0 on the evolution of the sources. These curves are obtained with $B_0 = 10^{12}$ G and $M_d \simeq 3.16 \times 10^{-6} M_\odot$, by changing P_0 only. It is seen in Fig. 2.1 that all the three paths (1), (2), and (3) described above can be produced with different P_0 values given in Fig. 1. The black dashed curves in the top panels of Figs.1-3 show the theoretical cooling luminosity of the neutron star. For $P_0 = 300$ ms (red curve), the star starts its evolution in the WP phase (path 1). For a slightly shorter initial period ($P_0 = 250$ ms), the neutron star cannot enter initially into the WP phase. The evolution starts in the SP phase in which accretion is not allowed. Due to efficient spin-down torque, the source can slow down to the critical period for the onset of accretion (path 2). From this point on, the evolution is similar to the path (1). In both cases, these illustrative sources spin down to periods of a few seconds until the WP/SP transitions. If P_0 is decreased further ($P_0 = 200$ ms for the purple curve), the star starts its evolution and always remain in the SP phase (path 2).

The Disk Mass, M_d. The model curves given in Fig. 2.2 are obtained by changing M_d only. For all these models, we employed $B_0 = 10^{12}$ G and $P_0 = 250$ ms. For the greatest M_d ($4.7 \times 10^{-6} M_\odot$), the star can initially enter into the WP phase and follows path 1 (red curve). For an intermediate M_d (blue curve), this particular source is born in the SP phase, and later ($t \sim 10^3$ yr) enter the WP phase switching off the radio pulses (path 3). During the long-lasting ($\sim 3 \times 10^4$ yr) WP phase, P increases to ~ 3 s. After termination of the accretion, the source enters into the SP phase (note that this curve is the same as the blue curve in Fig.2.1). For the smallest mass (path 2, purple curve), the system evolves always in the SP phase, like the source with the shortest P_0 in Fig. 2.1.

The Magnetic Dipole Field Strength, B_0. The model curves in Fig. 2.3 are obtained with different B_0 values ($P_0 = 200$ ms and $M_d \simeq 4.7 \times 10^{-6} M_\odot$ for the three models). The long-term evolution is more sensitive to B_0 in comparison with P_0 and M_d. For the strong B_0 (1×10^{13} G), the star can initially enter into the SP phase (path 3, blue curve), and later make a transition into the WP phase at $t \sim 10^4$ yr.
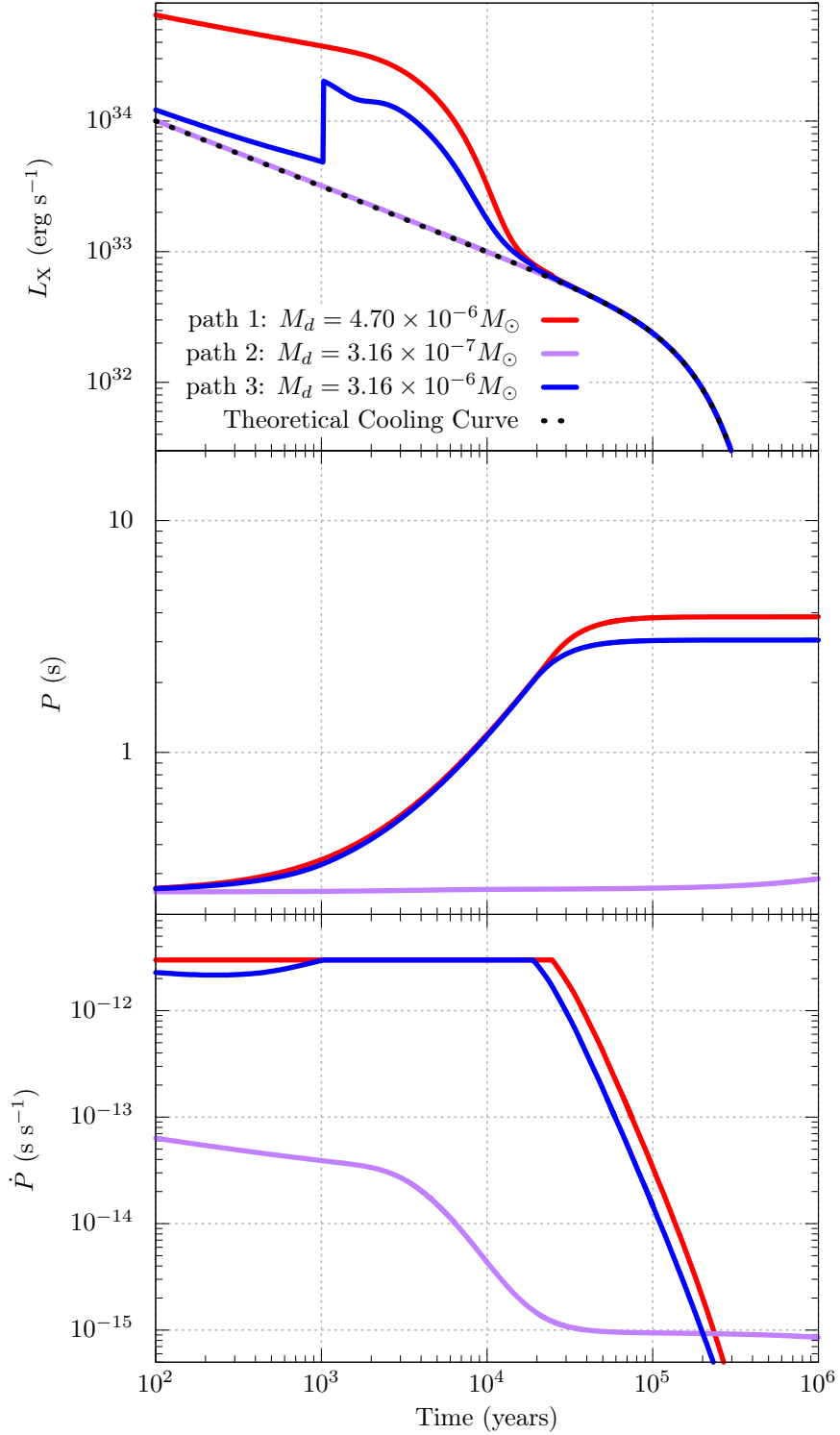
Figure 2.2 Illustrative model curves that show the effect of M_d on the long-term evolution. For these models, $B_0 = 10^{12}$ G and $P = 250$ ms. The M_d values are given in the top panel.

11
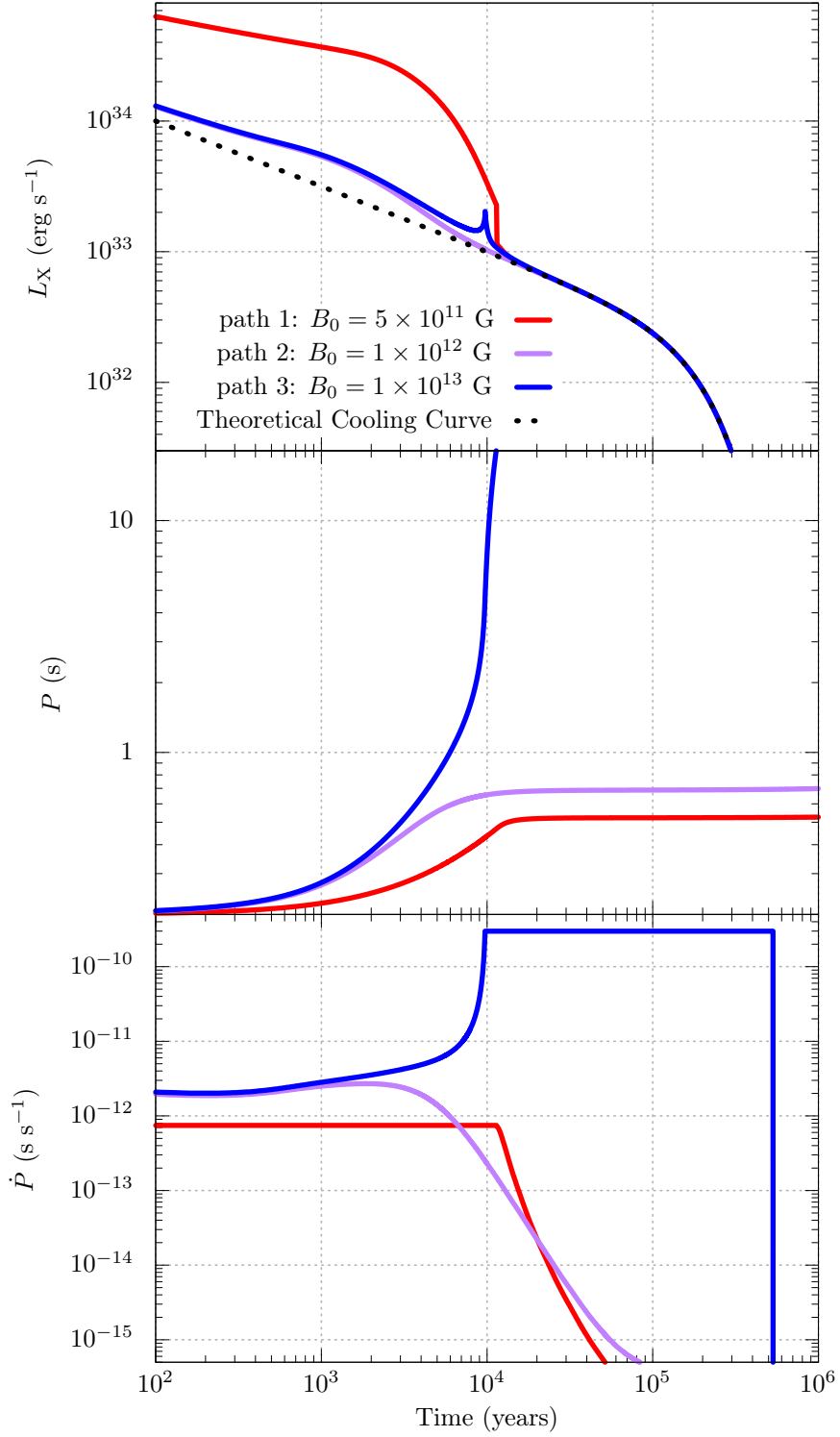
Figure 2.3 These model curves are obtained by changing B_0 only. The B_0 values are given in the top panel. For these models, we take $P_0 = 200$ ms and $M_d \simeq 4.7 \times 10^{-6} M_\odot$.

During the long-lasting WP phase, the source slows down and enters back into the SP phase at $t \sim 5 \times 10^5$ yr. For $B_0 = 1 \times 10^{12}$ G (purple curve), the system evolves always in the SP phase (path 2). For the weakest dipole field ($B_0 = 5 \times 10^{11}$ G), the evolution is initially in the WP phase until the WP/SP transition at $t \sim 10^4$ yr (path 1, red curve). The $\dot{P}$ value during the WP phase of path 1 is much smaller than in the WP phase of path 3. This is because $\dot{P} \propto B_0^2$ in the WP phase. The sources that have the same B_0 evolve with the same (maximum) $\dot{P}$ in the WP phase (see also Figs. 2.1 and 2.2).

It was shown in the earlier works that the individual source properties of AXP/SGRs, XDINs, HBRPs, CCOs, and RRATs can also be reproduced in this model by changing the initial conditions using very similar main disk parameters as illustrated in this chapter (see also chapter 1). The results of these analyses can be summarized as follows: AXP/SGRs are the sources with $B_0 \sim 10^{12} - 10^{13}$ G (Benli & Ertan, 2016). The rotational properties and L_x of most of the AXP/SGRs are reproduced in the WP phase. Known XDINs have $B_0 \sim (0.3 - 1.3) \times 10^{12}$ G and currently evolve in the SP phase (Ertan et al., 2014). These B_0 and observed P values place XDINs well below the pulsar death line after the WP/SP transition. In this model, XDINs are not capable of radiating pulsed radio emission. AXP/SGR and XDIN properties can be obtained with large ranges of M_d, and the results are not sensitive to P_0. HBRP properties are obtained with $B_0 \sim 10^{12} - 10^{13}$ G while the sources are evolving in the SP phase (Benli & Ertan, 2017). Unlike XDINs, their relatively strong B_0 and short P place them above the pulsar death line. Among these neutron star populations, CCOs have the weakest fields (a few $\times 10^9$ G) (Benli & Ertan, 2018b). Their very low $\dot{P}$ indicates that their current periods ($\sim 0.1 - 0.4$ s) are likely to be close to their initial periods. These sources are found to be in the WP phase at present, mainly due to their weak dipole fields. Among more than 100 confirmed RRATs, L_x is known for only one source (PSR J1819-1458), while P and $\dot{P}$ were measured for 34 sources. Recently, Gençali & Ertan (2020) estimated the field strengths of RRATs without X-ray information. Their results show that the B_0 range of RRATs ($B_0 \sim 7 \times 10^9 - 6 \times 10^{11}$ G) can fill the B_0 gap between the B_0 ranges of XDINs and CCOs. This means that, in this model, the properties of all the populations can be produced with a continuous B_0 distribution.

Recently, PSR J0726-2612 was detected with $P = 3.44$ s, $\dot{P} = 2.93 \times 10^{-13}$ s s^{-1}, and $L_x \simeq 4 \times 10^{32}$ erg s^{-1} for $d = 1$ kpc (Speagle et al., 2011; Viganò et al., 2013) which are similar to those of XDINs and HBRPs, while its characteristic age ($\sim 2 \times 10^5$ yr) is one order smaller than those of XDINs ($1 - 4 \times 10^6$ yr). Due to its pulsed radio emission and relatively high $\dot{P}$ value, PSR J0726-2612 is generally classified as an HBRP (Speagle et al., 2011; Olausen et al., 2013; Watanabe et al.,

2019). Recently, Rigoselli et al. (2019) proposed that this source could be the first XDIN with observable radio pulses due to convenient viewing geometry. In Chapter 3, we investigated the possible evolutionary paths of PSR J0726-2612 in the fallback disk model. We have found that the evolution of the source is similar to that of some of the HBRPs, rather than XDINs. The details of the model results are given in Chapter 3.

3.   Is PSR J0726−2612 a dim isolated neutron star progenitor?

Ş. Özcan, A. A. Gençali, Ü. Ertan

3.1 INTRODUCTION

X-ray dim isolated neutron stars (XDINs) form an isolated neutron star population among other young neutron star systems, namely anomalous X-ray pulsars (AXPs), soft gamma ray repeaters (SGRs), rotating radio transients (RRATs), high-B radio pulsars (HBRPs), and central compact objects (CCOs). At present, there are seven known XDINs characterized by their thermal X-ray emission with black-body temperatures ranging from 40 to 110 eV and low X-ray luminosities in the range of $10^{31} - 10^{32}$ erg s^{-1} (Haberl, 2007; Turolla, 2009; Kaplan & van Kerkwijk, 2011). Rotational periods of XDINs are in the 3 – 17 s range (Haberl et al., 2004; Haberl, 2004; Tiengo & Mereghetti, 2007; Kaplan & van Kerkwijk, 2009a,b; Hambaryan et al., 2017) similar to those of AXPs and SGRs. Their characteristic ages $\tau_c = P/2\dot{P} = (1-4) \times 10^6$ yr where P and $\dot{P}$ are the rotational period and the period derivative of the neutron star. The kinematic ages are estimated to be between a few 10^5 yr and 10^6 yr by Speagle et al. (2011) which are consistent with the estimated cooling ages of the sources (Page, 2009). Soft gamma bursts, shown by AXPs and SGRs, continuous pulsed radio emission, or short radio bursts seen from RRATs have not been observed from XDINs (Mereghetti, 2011).

With the assumption that XDINs evolve with purely magnetic dipole torques, the dipole field strengths are inferred to be $B_0 = 6.4 \times 10^{19}(P\dot{P})^{1/2} \sim$ a few 10^{13} G at the poles of the sources. These strong dipole fields place XDINs above the pulsar death line in the $B_0 - P$ plane (Haberl, 2007), while no pulsed radio emission has been detected from these sources yet. It was proposed that the non-detection of pulsed radio emission from XDINs could be due to narrow beaming of their radio emission (Haberl, 2005). Recently observed radio pulsar PSR J0726–2612 (hereafter J0726) was proposed to be a good candidate to be an XDIN with an observable radio beam (Rigoselli et al., 2019). For this source, $P = 3.44$ s, close to the minimum of XDIN periods, and $\dot{P} = 2.93 \times 10^{-13}$ s s^{-1}, which give a characteristic age of $\sim 2 \times 10^5$ yr. The distance estimated from the dispersion measure (Burgay et al., 2006) using the electron distribution model of Yao et al. (2017) gives $d \sim 3$ kpc. Nevertheless, the dispersion measure is likely to be effected by the Gould Belt (Popov et al., 2005) crossing the line of sight to J0726. If the source is located in the Gould Belt as suggested by Speagle et al. (2011), then $d \lesssim 1$ kpc. For the model calculations, we take $d = 1$ kpc which gives an X-ray luminosity $L_{\rm x} \simeq 4 \times 10^{32}$ erg s^{-1} and comparable to the rotational power $\dot{E} = I\Omega_*\dot{\Omega}_* = 2.8 \times 10^{32}$ erg s^{-1} of the source (Rigoselli et al., 2019; Viganò et al., 2013), where I is moment of inertia, Ω_* is the angular velocity of the neutron star and $\dot{\Omega}_*$ is its time derivative. Since the rotational properties and $L_{\rm x}$ of J0726 are in the ranges of those observed from HBRPs ($P =$

16

$0.15 - 6.7$ s, $\dot{P} = 2.33 \times 10^{-14} - 4.02 \times 10^{-12}$ s s^{-1}, $L_{\mathrm{x}} \simeq 10^{31} - 4 \times 10^{34}$ erg s^{-1}), the source is also classified as a HBRP (Speagle et al., 2011; Olausen et al., 2013; Watanabe et al., 2019).

After a supernova explosion, a fallback disc can be formed around the neutron star (Colgate, 1971; Michel, 1988; Chevalier, 1989; Perna et al., 2014). To explain the properties of AXPs, Chatterjee et al. (2000) proposed that these sources are evolving with fallback discs. It was proposed that emergence of different isolated neutron star populations could be explained if the properties of fallback discs are included in the initial conditions together with initial period and magnetic dipole moment (Alpar, 2001). Fallback discs were invoked to explain different rotational characteristics of isolated neutron stars that are not explained by evolutions with purely dipole torques (Marsden et al., 2001; Menou et al., 2001; Ekşi & Alpar, 2003; Yan et al., 2012; Fu & Li, 2013). Emission properties of the fallback discs were also studied extensively (Perna et al., 2000; Ertan et al., 2007). It was shown by Ertan et al. (2007) that the broad-band spectrum of 4U 0142+61 from the optical to mid-IR bands (Hulleman et al., 2000, 2004; Morii et al., 2005; Wang et al., 2006) can be accounted for by the emission from the entire disc surface. The fallback disc model proposed by Alpar (2001) was developed later including the effects of the X-ray irradiation, cooling luminosity, and inactivation of the disc in the long-term evolution (Ertan et al., 2009, 2014). When there is a fallback disc around the star, the spin-down torque arising from the interaction of the inner disc with the dipole field of the star usually dominates the magnetic dipole torque. In the fallback disc model, B_0 values are estimated to be one to three orders smaller than the values inferred from the dipole torque formula. The long-term evolution of XDINs and HBRPs with fallback discs was studied earlier by Ertan et al. (2014) and Benli & Ertan (2017, 2018a). The model can reproduce P, $\dot{P}$ and L_{x} of individual XDIN and HBRP sources with B_0 in the ranges of $(0.3 - 1.3) \times 10^{12}$ G for XDINs and $(0.3 - 6) \times 10^{12}$ G for HBRPs. These relatively weak fields together with the long periods place XDINs well below the pulsar death line (see Ertan et al., 2014, figure 4) in the $B_0 - P$ diagram (Chen & Ruderman, 1993), while HBRPs with relatively strong fields and/or short periods are located above the death line (Benli & Ertan, 2017, 2018a). In other words, in the fallback disc model, the lack of radio pulses from XDINs is due to their weak dipole fields, rather than the beaming geometry.

In this work, our aim is to investigate the long-term evolution of J0726, and compare its properties and evolution with those of XDINs and HBRPs in the fallback disc model. The same model was applied earlier to AXP/SGRs, CCOs, and RRATs as well (Ertan et al., 2007, 2009, 2014; Çalışkan et al., 2013; Benli & Ertan, 2017; Gençali & Ertan, 2018). In Section 2, we briefly describe this model. We discuss the

results of model calculations in Section 3, and summarize our conclusions in Section 4.

3.2 THE MODEL

Since the details of the model calculations and its applications to different neutron star populations are given in earlier works (see e.g. Ertan et al., 2009, 2014; Benli & Ertan, 2016), we briefly describe the model calculations here.

We solve the disc diffusion equation starting with a surface density profile of a steady disc using the kinematic viscosity $\nu = \alpha c_{\mathrm{s}} h$ where, α is the kinematic viscosity parameter, c_{s} is the local sound speed, and h is the pressure scale height of the disc (Shakura & Sunyaev, 1973). In the accretion with spin-down (ASD) phase, we calculate the disc torque, N_{D}, acting on the star by integrating the magnetic torques from the conventional Alfvén radius, $r_{\mathrm{A}} \simeq (GM)^{-1/7} \mu^{4/7} \dot{M}_{\mathrm{in}}^{-2/7}$ (Lamb et al., 1973; Davidson & Ostriker, 1973), to the co-rotation radius, $r_{\mathrm{co}} = (GM/\Omega_*^2)^{1/3}$ where G is the gravitational constant, M is the mass of the neutron star and μ is its magnetic dipole moment, $\dot{M}_{\mathrm{in}}$ is the mass inflow-rate at the inner disc. The magnitude of this torque could be written in terms of $\dot{M}_{\mathrm{in}}$ and r_{A} as $N_{\mathrm{D}} = \frac{1}{2} \dot{M}_{\mathrm{in}} (GMr_{\mathrm{A}})^{1/2} \Big[1 - (r_{\mathrm{A}}/r_{\mathrm{co}})^3 \Big]$ (see Ertan & Erkut, 2008, for details). The contributions of the magnetic dipole torque, N_{dip}, and the spin-up torque associated with accretion on to the star, N_{acc}, are negligible in the long-term accretion regime of XDINs (Ertan et al., 2014). That is, the total torque acting on the star $N_{\mathrm{TOT}} = N_{\mathrm{D}} + N_{\mathrm{dip}} + N_{\mathrm{acc}}$ is dominated by N_{D} in the ASD phase of XDINs. In this regime, $r_{\mathrm{co}} < r_{\mathrm{A}} < r_{\mathrm{LC}}$, where $r_{\mathrm{LC}} = c/\Omega_*$ is the light cylinder radius, and c is the speed of light.

During the ASD phase, r_{A} increases with gradually decreasing $\dot{M}_{\mathrm{in}}$, and eventually becomes equal to r_{LC}. For $\dot{M}_{\mathrm{in}}$ below this critical value, we replace r_{A} with r_{LC} in the N_{D} equation. In the model, $r_{\mathrm{A}} = r_{\mathrm{LC}}$ is also the condition for the propeller-accretion transition. Since $\dot{M}_{\mathrm{in}}$ enters a sharp decay phase at the end of the ASD phase, exact value of $\dot{M}_{\mathrm{in}}$ for the accretion-propeller transition does not affect our results significantly. In the strong-propeller (SP) phase, we assume that all the matter inflowing to the inner disc is expelled from the system. The pulsed radio emission is allowed only in the SP phase when there is no accretion on to the source.

In the ASD phase, the mass accretion on to the star produces an X-ray luminosity, $L_{\mathrm{acc}} = GM\dot{M}_*/R_*$, where R_* is the radius of the neutron star. In this

phase, we take the mass accretion rate $\dot{M}_* = \dot{M}_{\text{in}}$. The total X-ray luminosity, $L_{\text{x}} = L_{\text{acc}} + L_{\text{cool}}$, where L_{cool} is the intrinsic cooling luminosity of the star (Page, 2009). In the L_{cool} calculation, we also include the small contribution of the external torques to the internal heating of the neutron star (Alpar, 2007). In the SP phase, $\dot{M}_* = 0$, $N_{\text{acc}} = 0$, and $L_{\text{x}} = L_{\text{cool}}$, since accretion is not allowed in this regime. The disc is heated by X-ray irradiation in addition to the viscous dissipation. The effective temperature of the disc can be written as $T_{\text{eff}} \simeq \left[(D + F_{\text{irr}})/\sigma \right]^{1/4}$ where D is the rate of viscous dissipation per unit area of the disc, σ is the Stefan-Boltzmann constant, $F_{\text{irr}} = 1.2 C L_{\text{x}}/(\pi r^2)$ is the irritation flux, where r is the radial distance from the star, C is the irradiation parameter, which depends on the albedo and geometry of the disc surfaces (Fukue, 1992). The disc becomes viscously inactive below a critical temperature, T_{p}. Dynamical outer radius, r_{out}, of the viscously active disc is equal to the radius currently at which $T_{\text{eff}} = T_{\text{p}}$. Across the outer disc, F_{irr} dominates D, that is, the X-ray irradiation significantly affects the long-term evolution of the source by extending the life-time of the active disc.

The main disc parameters (α, C, T_{p}) for the fallback discs of different neutron star populations are expected to be similar. The same model employed here can reproduce the individual source properties of AXP/SGRs, CCOs, HBRPs and XDINs with $T_{\text{p}} \sim (50 - 150)$ K, and C $= (1 - 7) \times 10^{-4}$ (Ertan & Çalışkan, 2006; Ertan et al., 2007; Çalışkan et al., 2013; Ertan et al., 2014; Benli & Ertan, 2016, 2017, 2018a,b). These T_{p} values in the model are in good agreement with the results of the theoretical work indicating that the disc is likely to be active at very low temperatures (Inutsuka & Sano, 2005). The range of C estimated in our model is similar to that estimated from the optical and X-ray observations of the low-mass X-ray binaries (see e.g. Dubus et al., 1999). We try to obtain the properties of J0726 also with these main disc parameters. This provides a systematic comparison between the initial conditions of different populations, namely the magnetic dipole field strength B_0, the initial disc mass M_{d}, and the initial period P_0.

The α parameter does not significantly affect the long-term evolution. The conditions in a slowly evolving fallback disc are similar to steady-state conditions. The outer regions of the active disc govern the rate of mass-flow to the inner disc. That is, the α parameter in our model should be considered as the property of the outer disc. T_{p} and C are degenerate parameters. With smaller T_{p} values the active disc has a longer lifetime. A stronger irradiation (greater C) also extends the lifetime of the active disc. A detailed discussion about the effects of these parameters on the evolution of the neutron star can be found in Ertan et al. (2009).

3.3 RESULTS AND DISCUSSION

The model curves seen in Fig. 3.1 illustrate two different evolutionary histories for J0726: (1) The model source following curve 1 starts its evolution in the ASD phase with $L_{\mathrm{x}} \simeq L_{\mathrm{acc}}$, and remains in this phase until it makes a transition to the SP phase at $t \sim 3 \times 10^4$ yr. The solid and dashed branches of the curves correspond to the ASD and SP phases respectively. It is seen in the middle and bottom panels that the rapid increase of P stops with sharply decreasing $\dot{P}$ after the ASD/SP transition. (2) Curve 2 represents the evolution of a neutron star that remains always in the SP phase with $L_{\mathrm{x}} \simeq L_{\mathrm{cool}}$. For a given B_0, the sources with M_{d} smaller than a critical value cannot enter the ASD phase, and evolves in the SP phase likely as radio pulsar. The rotational evolution for this type of evolution is sensitive to M_{d}, while for type (1) solution, P and $\dot{P}$ evolution do not significantly depend on M_{d} (see e.g. Benli & Ertan, 2016).

Illustrative model curves seen in Fig. 3.1 are obtained with the main disc parameters: $\alpha = 0.045$, $T_{\mathrm{p}} = 100$ K, $C = 1 \times 10^{-4}$. The initial conditions for curve 1 are $P_0 = 0.3$ s, $M_{\mathrm{d}} = 1.1 \times 10^{-5}$ $M_{\odot}$, $B_0 = 9 \times 10^{11}$ G. The maximum B_0 allowed for the type (1) solution (curve 1) is $\sim 1.2 \times 10^{12}$ G, while the type (2) solution can reproduce the source properties with $B_0 \gtrsim 1.5 \times 10^{12}$ G. For $P = 3.44$ s, the minimum B_0 required for the pulsed radio emission is $\sim 1.4 \times 10^{12}$ G. In Fig. 3.2, we have also plotted the evolution of $\dot{M}_*$, r_{A}, r_{co} and r_{LC} in the ASD phase of type (1) solution. Due to the simplifications in our model, we cannot exclude type (1) evolution. Nevertheless, even if the source is inside the death valley, it is too close to the death line, which implies that this solution is not very likely to represent the actual evolution of J0726. Most of the radio pulsars seem to die inside the death valley at points not very close to the pulsar death line. Otherwise, if the sources switch off the radio pulses when crossing the death line, their number density would increase close to the death line, which is not observed. Some of the sources die close to the upper boundary, while some others close to the lower boundary (death line), altogether forming a roughly homogeneous distribution inside the death valley. For our type (1) solution, after termination of the ASD phase, the source finds itself very close to the lower boundary. In this case, the star can show radio pulses only if its actual death point is indeed very close to the lower boundary. Type (2) solution seems to be more reasonable representation of the evolution of J0726. This evolution is similar to those of some of the HBRPs in the same model (Benli & Ertan, 2017, 2018a). For both solutions, the source is currently evolving in the SP phase at an age $\sim 5 \times 10^4$ yr. At present, the star is slowing down dominantly by the disc torque that will eventually decrease below the magnetic dipole torque at $t \sim$ a few
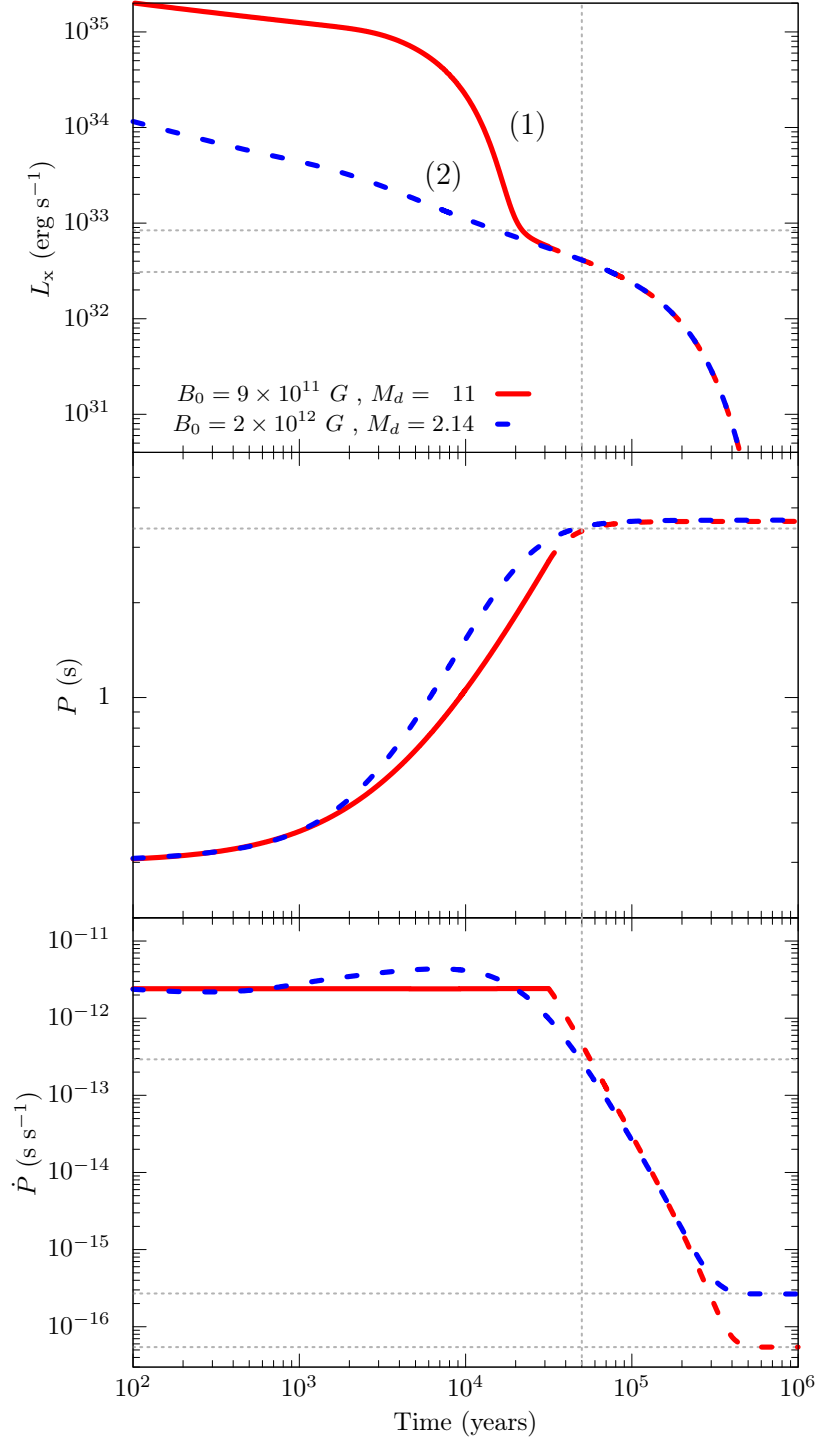
Figure 3.1 Illustrative model curves for the long-term evolution of PSR J0726–2612. The curves are obtained with B_0 and M_d (in units of 10^{-6} $M_\odot$) values given in the top panel. The main disc parameters employed in both models are $C = 1 \times 10^{-4}$, $T_p = 100$ K, and $\alpha = 0.045$. Horizontal lines show the observed $P = 3.44$ s, $\dot{P} = 2.93 \times 10^{-13}$ s s^{-1}, and the estimated L_x range for $d = 1$ kpc (Rigoselli et al., 2019). For curve 1, solid and dashed branches correspond to the ASD and SP phases respectively. For the evolution represented by curve 2, the source always remains in the SP phase, and this curve is a more likely representation of the evolution of PSR J0726–2612 (see the text for details). Eventually, $\dot{P}$ curves converge to the levels corresponding to the magnetic dipole torques (shown by two horizontal dotted lines at the bottom of the $\dot{P}$ panel).
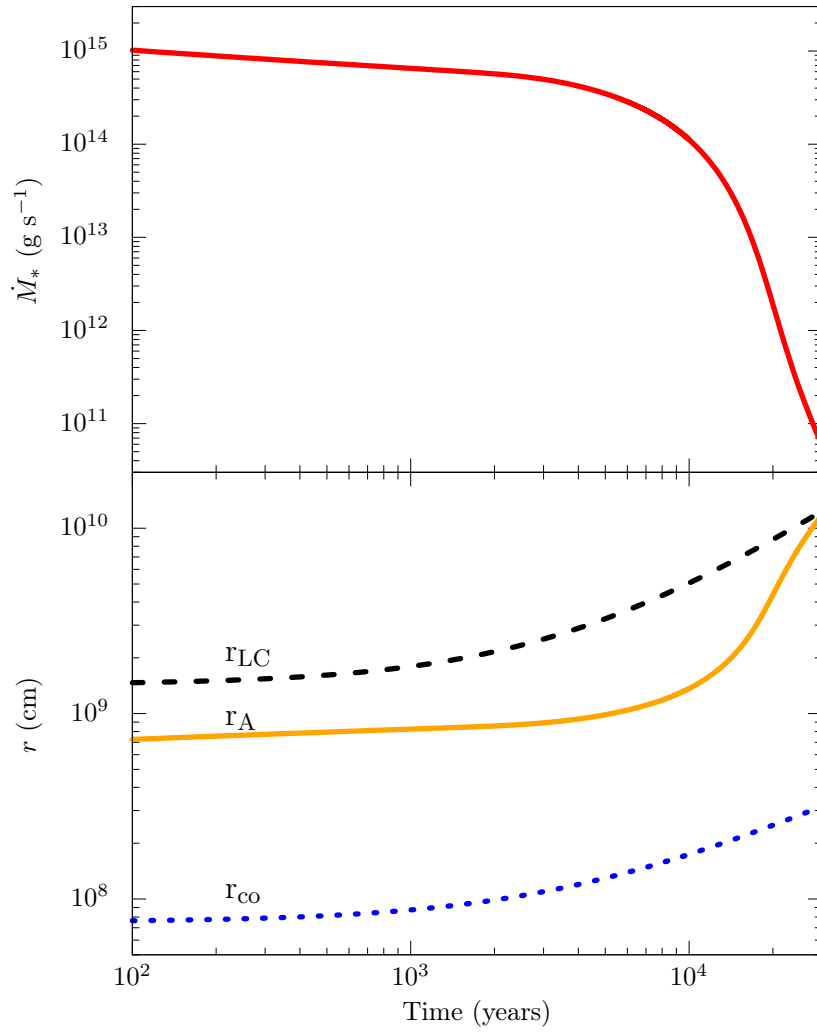
Figure 3.2 The evolution of the accretion rate, r_{co}, r_{A} and r_{LC} in the ASD phase of type (1) evolution (see Fig. 3.1). The accretion is switched off at $t \simeq 3 \times 10^4$ s, and the system enters the SP phase (see the text).

$\times 10^5$ yr. For instance, for $B_0 = 2 \times 10^{12}$ G, (curve 2) the sharp decrease in $\dot{P}$ will continue down to $\dot{P} \simeq 2.7 \times 10^{-16}$ s s^{-1}. Our results indicate that J0726 will evolve to these ages with a $\dot{P}$ that is about three orders of magnitude smaller than its present value (Fig. 3.1). This means that the source is likely to be classified as a normal radio pulsar with $B_0 \sim$ a few $\times 10^{12}$ G deduced from P and $\dot{P}$ at the ages of XDINs. In Fig. 3.3, we have plotted the evolution of J0726 in the $P - \dot{P}$ and $P - B_0$ diagrams together with XDINs and HBRPs with the properties estimated in our model.

In our present and earlier works, we employed theoretical cooling curve estimated by Page (2009) for conventional dipole fields. This cooling curve could differ from the actual cooling curve depending on some unknown details of the neutron star properties like equation of state and mass of the star (see e.g. Potekhin & Chabrier, 2018; Potekhin et al., 2020). For the sources that are currently in the ASD phase, the details of the cooling curve do not affect our results, but could modify our model parameters for sources in the SP phase, like XDINs. The ages of XDINs estimated in our model are on the average a few times smaller than the estimated kinematic ages. If the actual ages are indeed close to the kinematic ages, the source properties can be obtained with B_0 values smaller than we reported here and in Ertan et al. (2014) by a factor smaller than two. The field strengths estimated in our model should be considered taking these uncertainties into account. These small changes in B_0 do not change the qualitative features of the model curves for XDINs. Recently, the period of RX J0720.4–3125 was updated from 8.39 s to 16.78 s by Hambaryan et al. (2017). The period derivative of the source was also updated from $\sim 7 \times 10^{-14}$ s s^{-1} to 1.86×10^{-13} s s^{-1} by Hambaryan & Neuhäuser (2017). For this source, we have performed new simulations and modified the model parameters obtained by Ertan et al. (2014). Our results and model parameters are given in Fig. 3.4. With the updated period and period derivative, using the same main disc parameters as employed in Ertan et al. (2014), the model can reproduce the source properties with slightly higher B_0 $((1.3 - 1.8) \times 10^{12}$ G) values in comparison with the B_0 obtained in Ertan et al. (2014). Similar results could be produced for a large range of disc masses.

In our model, the inner disc interacts with the large-scale magnetic dipole field of the neutron star. Close to the surface of the star, there could be quadrupole magnetar fields which could affect the surface temperature distribution and the absorption features (Güver et al., 2011). Presence of these small-scale strong fields in XDINs and other isolated neutron star populations is compatible with the fallback

---

[1]https://www.atnf.csiro.au/research/pulsar/psrcat/
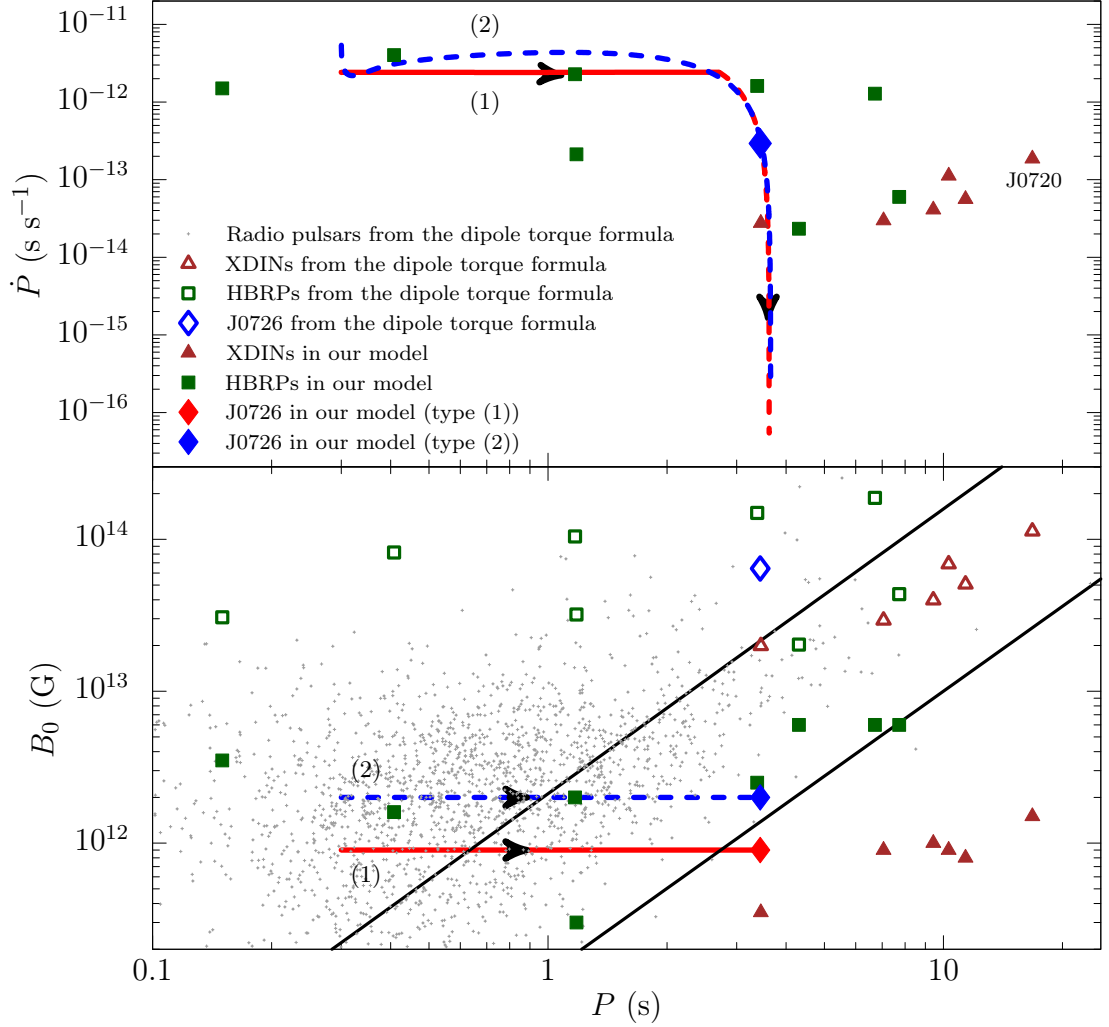
Figure 3.3 Long-term evolution in the $P - \dot{P}$ and $B_0 - P$ diagrams for the same model curves given in Fig. 3.1. XDINs and HBRPs are indicated by triangles and squares respectively. In the $B_0 - P$ plane, empty symbols show B_0 values inferred from the dipole torque formula using P and $\dot{P}$ values (ATNF Pulsar Catalogue version 1.63, Manchester et al., 2005)[1]. The filled symbols indicate the average B_0 values estimated in our model (Ertan et al., 2014; Benli & Ertan, 2017, 2018a). The solid lines are the upper and lower borders of the pulsar death valley (Chen & Ruderman, 1993). The filled diamonds show the current location of J0726 estimated for type (1) and type (2) solutions.
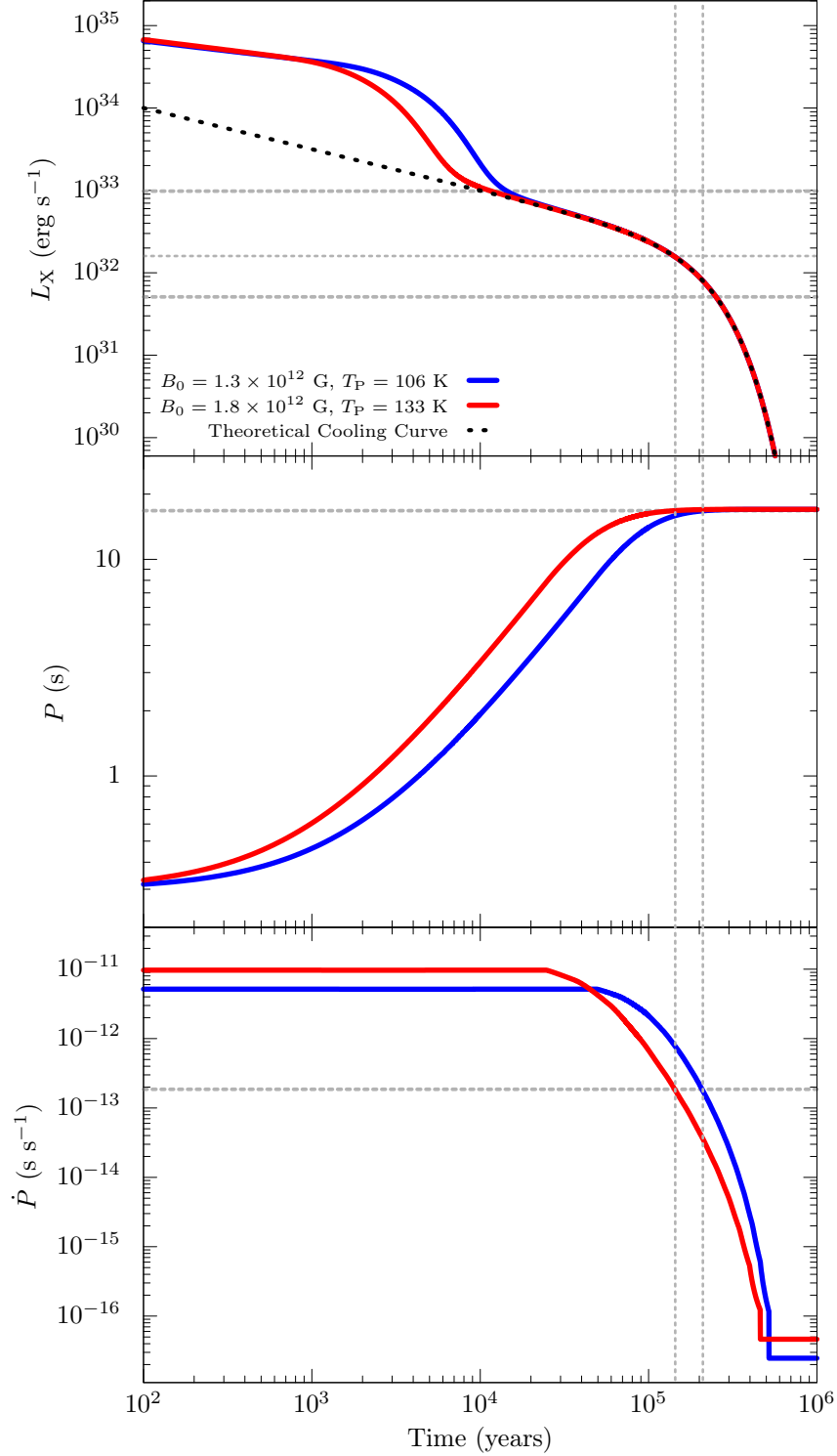
Figure 3.4 Illustrative model curves for the long-term evolution of RX J0720.4—3125 with the updated period and period derivative. For both models, $\alpha = 0.045$, $C = 1 \times 10^{-4}$, $P_0 = 0.3$ s, $M_d = 4.74 \times 10^{-6} M_\odot$. The curves obtained with B_0 and T_p values given in the top panel. The dotted curve indicates the theoretical cooling curve (Page, 2009). Horizontal dashed lines show $P = 16.78$ s, $\dot{P} = 1.86 \times 10^{-13}$ s s^{-1}, $L_x = 1.6 \times 10^{32}$ erg s^{-1} as used in Ertan et al. (2014) assuming $d = 270$ pc. There is a large uncertainty in $d = 280^{+210}_{-85}$ pc (Eisenbeiss, 2011; Tetzlaff et al., 2011; Hambaryan et al., 2017).

25

disc model, nevertheless these detailed surface properties are not addressed in our long-term evolution model. Some other spectral features that could be produced by the disc-field interaction should also be studied independently. In particular, Ertan (2017) showed that the heating of the inner disc boundary by the magnetic stresses can account for the optical/UV excesses of XDINs, while the entire disc spectra are consistent with the observed upper limits in the IR bands. We note that there is an uncertainty in the disk spectrum because of unknown inclination angle of the disk. To estimate the entire disk spectrum, at least a single detection in one of the IR bands is needed. At present, there is no IR/optical detection or upper limits estimated for J0726.

The X-ray luminosities of XDINs exceed their spin-down powers. In our long-term evolution model, this is a natural outcome of rapid increase in periods by efficient disc torques and sharp decrease in $\dot{P}$ in the late SP phase, which leaves the observed spin-down powers below the cooling luminosities of these sources. The current periods of XDINs together with the weak fields estimated in our model place these sources below the pulsar death line (Ertan et al., 2014, plotted also in Fig. 3.3). This indicates that known XDINs cannot emit radio pulses in our model. There are a few exceptional active radio pulsars that are close to, but below the death line, namely PSR J0250+5854 with $P = 23.5$ s (Tan et al., 2018), PSR J2251–3711 with $P = 12.1$ s (Morello et al., 2020), PSR J2144–3933 with $P = 8.5$ s (Young et al., 1999). Nevertheless, in our model, we find the locations of XDINs well below the death line where there are no radio pulsars.

Is it possible that a source with $B_0 \sim$ a few $\times 10^{12}$ G starts in the ASD phase with a greater M_d? It is possible, and we estimate that these sources become AXP/SGRs, and evolve to relatively long periods which leave them below the pulsar death line at the end of the ASD phase. In our model, these sources can never become radio pulsar in their lifetimes provided that the accretion is not hindered occasionally due to instabilities at the inner disc.

3.4 CONCLUSIONS

We have shown that P, $\dot{P}$ and L_x of J0726 can be achieved by a neutron star evolving with a fallback disc. We have found that there are two possible evolutionary histories that could produce the properties of J0726. For both solutions, the source is in the strong-propeller (SP) phase at present. In the first alternative (curve 1 in

Fig. 3.1), the star initially evolves in the accretion with spin-down (ASD) phase, and makes a transition into the SP phase at an earlier time of its evolution. For the second type of solution (curve 2 in Fig. 3.1), the source always evolves in the SP phase. Since the X-ray luminosity is powered by the cooling luminosity in the SP phase, the model sources reach the properties of J0726 at an age close to the estimated cooling age ($\sim 5 \times 10^4$ yr) of J0726.

The radio pulsars following the type (1) evolution are not likely to be common, since these sources find themselves very close to the pulsar death line after the accretion is switched off. The curve 2 seems to show a more likely evolution for J0726 which is also similar to the evolution of some of the HBRPs, rather than XDINs. The model curves indicate that the source will acquire the rotational properties of normal radio pulsars at the ages of XDINs (Fig. 3.1).

In our long-term evolution model, the basic difference between the HBRPs and XDINs are the field strengths B_0. XDINs with relatively small B_0 ($10^{11} - 10^{12}$ G) tend to start their evolution in the ASD phase, since it is easier for the inner disc to extend down to the co-rotation radius for weaker dipole fields. On the other hand, HBRPs with stronger fields ($B_0 \gtrsim 2 \times 10^{12}$ G) either always evolve in the SP phase, as we estimate for J0726, or make a transition from the initial SP phase to the ASD phase at a later time of evolution. In the latter case, the sources are expected to evolve to the properties of AXP/SGRs (Benli & Ertan, 2017). A detailed comparison of the long-term evolutions and the statistical properties of these neutron star populations in the fallback disc model will be studied in an independent work.

4.   DISCUSSION AND CONCLUSIONS

In this thesis, we first investigated the dependence of the long-term evolution of neutron stars with fallback disks on the initial conditions P_0, M_d and B_0. There are three basic evolutionary paths that could be followed by a neutron star in this model. We have shown that all these three paths can be produced by changing either of the three initial conditions. The model curves are found to be more sensitive to B_0 in comparison with P_0 and M_d. A given model source follows path 1 (WP+SP), path 2 (SP) or path 3 (SP+WP+SP) depending on the chosen set of initial conditions (see Chapter 2 for the description of the paths). The sources with relatively long P_0 and/or high M_d are more likely to enter the WP phase initially, or at a later time of evolution for a given B_0. Dependence of the evolution on B_0 is more complicated. A neutron star with a weaker dipole field can enter the WP phase more easily for given P_0 and M_d. On the other hand, the sources with relatively strong fields, which are not likely to start the evolution in the WP phase, tend to evolve with increasing $\dot{P}$, and eventually to make a transition to the WP phase at a later time (path 3). For sources starting its evolution in the SP phase with intermediate fields, $\dot{P}$ usually decreases in time leaving the source always in the SP phase (path 2) (see Chapter 2).

In the fallback disk model, AXP/SGRs and XDINs are the sources reaching their long periods in the WP phase of either path 1 (WP+SP) or path 3 (SP+WP+SP). AXP/SGRs have dipole fields ($B_0 \sim 10^{12-13}$ G) stronger than those of XDINs ($B_0 \sim 10^{11-12}$ G). Most of the AXP/SGRs are in the WP phase at present, while XDINs are slowing down with the disk torques in the final SP phase. The estimated B_0 values for HBRPs are similar to those of AXP/SGRs. HBRPs could be following either path 3 (SP+WP+SP) or path 2 (Always SP). In both cases, the sources can be identified as HBRPs during the initial phases of the evolution (when they have high $\dot{P}$ values in the SP phase). Among the single neutron star populations, CCOs seem to have the weakest dipole fields (a few 10^9 G). Depending on P_0 and M_d values, a fraction of these sources could experience a short-lasting initial spin-up phase followed by a WP phase, while for the remaining fraction, evolution

starts in the WP phase (Benli & Ertan, 2018b). These sources evolve following path 1 (WP+SP). Simple statistical calculations imply that RRATs, together with XDINs, have the highest birth rates among these neutron star populations. Nevertheless, except one source, the X-ray luminosities of RRATs are not known. Recently, Gençali & Ertan (2020) estimated the field strengths of RRATs with known $\dot{P}$ values. Their results show that the B_0 range of RRATs ($\sim 7 \times 10^9 - 6 \times 10^{11}$ G) could fill the B_0 gap between the B_0 values of XDINs and CCOs estimated in the same model. In other words, the X-ray and rotational properties of these neutron star populations can be reproduced with a continuous B_0 distribution in the fallback disk model.

These results indicate that all isolated neutron star populations can be explained in the fallback disk model. The energies and the short time-scales of the soft gamma burst of AXP/SGRs require strong (magnetar) fields, much stronger than the B_0 values estimated in the fallback disk model. Nevertheless, it is not required that these magnetar fields are stored in the dipole components. Strong, small-scale quadropole fields located close to the surface of the star, can also power these bursts. Since the inner disk interacts with the large-scale dipole component of the neutron star, presence of strong higher multipoles is compatible with the fallback disk model. The discovery of low-B magnetars (SGR 0418+5729 and Swift J1822.3-1606) (Turolla et al., 2011; Rea et al., 2012), indeed showed that SGR bursts do not require magnetar dipole fields.

An important difference between the predictions of the magnetar and the fallback disk models is about the pulsed radio emission from XDINs which are estimated to have a birth rate comparable to that of normal radio pulsars. Radio pulsar behaviour is not expected from these sources in the fallback disk model, while the non-detection of radio pulses is assumed to be due to narrow beaming of the radio emission in the magnetar model. Recently discovered radio pulsar PSR J0726-2612 which, apparently, seems to evolve towards the XDIN properties, raised the debate on whether this source could be the first XDIN with observable radio pulses (Rigoselli et al., 2019). In the second part of this thesis, we have investigated the long-term evolution of this source in the frame of the fallback disk model described in Chapter 2. Our results are summarized below.

We have shown that the X-ray and the rotational properties of PSR J0726-2612 can be achieved by a neutron star evolving with a fallback disk. We have found that there are two basic evolutionary avenues leading to the source properties, which correspond to evolutionary path 1 (WP+SP) and path 2 (SP) described in Chapter 2. The solution that gives path 1 is not consistent with the radio pulsar behaviour of the source, since the allowed B_0 values ($\lesssim 1.2 \times 10^{12}$ G) for this solution place the

source below the pulsar death line. The evolution following path 2 (always in the SP phase) is a typical evolutionary curve for some HBRPs and requires $B_0 \gtrsim 2 \times 10^{12}$ G, for which the source remains above the pulsar death line. This solution produces the P, $\dot{P}$, and L_x of the source simultaneously at an age $\sim 5 \times 10^4$ yr. The source seems to be much younger than XDINs which have kinematic ages of several 10^5 yr. At present, this system has HBRP properties and is approaching the features of a normal radio pulsar. Our results imply that PSR J0726-2612 will never become an XDIN, and that this source will be identified as normal radio pulsar at the ages of XDINs.

These results motivate us to try to reproduce the properties of all isolated neutron star populations using a single set of disk parameters in a single picture, and to determine the detailed evolutionary links of these systems in the fallback disk model. This will be the subject of the future work on these systems.

BIBLIOGRAPHY

Abdo, A. A., Ajello, M., Allafort, A., et al. 2013, The Astrophysical Journal Supplement, 208, 17, doi: 10.1088/0067-0049/208/2/17

Alpar, M. A. 2001, The Astrophysical Journal, 554, 1245, doi: 10.1086/321393

—. 2007, Applied Surface Science, 308, 133, doi: 10.1007/s10509-007-9376-0

Alpar, M. A., Cheng, A. F., Ruderman, M. A., & Shaham, J. 1982, Nature, 300, 728, doi: 10.1038/300728a0

Alpar, M. A., Ertan, Ü., & Çalışkan, Ş. 2011, The Astrophysical Journal Letters, 732, L4, doi: 10.1088/2041-8205/732/1/L4

Baade, W., & Zwicky, F. 1934, Proceedings of the National Academy of Science, 20, 259, doi: 10.1073/pnas.20.5.259

Bachetti, M., Harrison, F. A., Walton, D. J., et al. 2014, Nature, 514, 202, doi: 10.1038/nature13791

Benli, O., & Ertan, Ü. 2016, Monthly Notices of the Royal Astronomical Society, 457, 4114, doi: 10.1093/mnras/stw235

—. 2017, Monthly Notices of the Royal Astronomical Society, 471, 2553, doi: 10.1093/mnras/stx1735

—. 2018a, New Astronomy, 61, 78, doi: 10.1016/j.newast.2017.12.005

—. 2018b, Monthly Notices of the Royal Astronomical Society, 478, 4890, doi: 10.1093/mnras/sty1399

Bhalerao, V., Romano, P., Tomsick, J., et al. 2015, Monthly Notices of the Royal Astronomical Society, 447, 2274, doi: 10.1093/mnras/stu2495

Bondi, H., & Hoyle, F. 1944, Monthly Notices of the Royal Astronomical Society, 104, 273, doi: 10.1093/mnras/104.5.273

Burderi, L., & D'Amico, N. 1997, The Astrophysical Journal, 490, 343, doi: 10.1086/304846

Burgay, M., Joshi, B. C., D'Amico, N., et al. 2006, Monthly Notices of the Royal Astronomical Society, 368, 283, doi: 10.1111/j.1365-2966.2006.10100.x

Çalışkan, Ş., Ertan, Ü., Alpar, M. A., Trümper, J. E., & Kylafis, N. D. 2013, Monthly Notices of the Royal Astronomical Society, 431, 1136, doi: 10.1093/mnras/stt234

Cameron, A. G. 1959, The Astrophysical Journal, 130, 884, doi: 10.1086/146780

Chadwick, J. 1932, Nature, 129, 312, doi: 10.1038/129312a0

Chatterjee, P., Hernquist, L., & Narayan, R. 2000, The Astrophysical Journal, 534, 373, doi: 10.1086/308748

Chen, K., & Ruderman, M. 1993, The Astrophysical Journal, 402, 264, doi: 10.1086/172129

Chevalier, R. A. 1989, The Astrophysical Journal, 346, 847, doi: 10.1086/168066

Colgate, S. A. 1971, The Astrophysical Journal, 163, 221, doi: 10.1086/150760

Davidson, K., & Ostriker, J. P. 1973, The Astrophysical Journal, 179, 585, doi: 10.1086/151897

Dubus, G., Lasota, J.-P., Hameury, J.-M., & Charles, P. 1999, Monthly Notices of the Royal Astronomical Society, 303, 139, doi: 10.1046/j.1365-8711.1999.02212.x

Duncan, R. C., & Thompson, C. 1992, The Astrophysical Journal Letters, 392, L9, doi: 10.1086/186413

Eisenbeiss, T. 2011, PhD thesis, submitted, AIU, Friedrich-Schiller-Universität Jena, Germany

Ekşi, K. Y., & Alpar, M. A. 2003, The Astrophysical Journal, 599, 450, doi: 10.1086/379193

Ertan, Ü. 2017, Monthly Notices of the Royal Astronomical Society, 466, 175, doi: 10.1093/mnras/stw3131

Ertan, Ü., & Çalışkan, Ş. 2006, The Astrophysical Journal Letters, 649, L87, doi: 10.1086/508347

Ertan, Ü., Çalışkan, Ş., Benli, O., & Alpar, M. A. 2014, Monthly Notices of the Royal Astronomical Society, 444, 1559, doi: 10.1093/mnras/stu1523

Ertan, Ü., Ekşi, K. Y., Erkut, M. H., & Alpar, M. A. 2009, The Astrophysical Journal, 702, 1309, doi: 10.1088/0004-637X/702/2/1309

Ertan, Ü., & Erkut, M. H. 2008, The Astrophysical Journal, 673, 1062, doi: 10.1086/524679

Ertan, Ü., Erkut, M. H., Ekşi, K. Y., & Alpar, M. A. 2007, The Astrophysical Journal, 657, 441, doi: 10.1086/510303

Frank, J., King, A., & Raine, D. J. 2002, Accretion Power in Astrophysics: Third Edition (Cambridge University Press)

Fu, L., & Li, X.-D. 2013, The Astrophysical Journal, 775, 124, doi: 10.1088/0004-637X/775/2/124

Fukue, J. 1992, Publications of the Astronomical Society of Japan, 44, 663

Gavriil, F. 2008, Magnetar Emission from Highly Magnetized Rotation-Powered Pulsars, RXTE Proposal

Gençali, A. A., & Ertan, Ü. 2018, Monthly Notices of the Royal Astronomical Society, 481, 244, doi: 10.1093/mnras/sty2287

—. 2020, Monthly Notices of the Royal Astronomical Society, 500, 3281, doi: 10.1093/mnras/staa3371

Giacconi, R., Gursky, H., Kellogg, E., Schreier, E., & Tananbaum, H. 1971, The Astrophysical Journall, 167, L67, doi: 10.1086/180762

Gotthelf, E. V., Halpern, J. P., & Alford, J. 2013, The Astrophysical Journal, 765, 58, doi: 10.1088/0004-637X/765/1/58

Güver, T., Göğüş, E., & Özel, F. 2011, Monthly Notices of the Royal Astronomical Society, 418, 2773, doi: 10.1111/j.1365-2966.2011.19677.x

Haberl, F. 2004, Advances in Space Research, 33, 638, doi: 10.1016/j.asr.2003.07.022

Haberl, F. 2005, in 5 years of Science with XMM-Newton, ed. U. G. Briel, S. Sembay, & A. Read, 39–44

—. 2007, Applied Surface Science, 308, 181, doi: 10.1007/s10509-007-9342-x

Haberl, F., Motch, C., Zavlin, V. E., et al. 2004, Astronomy & Astrophysics, 424, 635, doi: 10.1051/0004-6361:20040440

Hambaryan, V., & Neuhäuser, R. 2017, in Astronomical Society of the Pacific Conference Series, Vol. 511, Non-Stable Universe: Energetic Resources, Activity Phenomena and Evolutionary Processes (San Francisco: Astronomical Society of the Pacific,), 51–58

Hambaryan, V., Suleimanov, V., Haberl, F., et al. 2017, Astronomy & Astrophysics, 601, A108, doi: 10.1051/0004-6361/201630368

Hewish, A., Bell, S. J., Pilkington, J. D. H., Scott, P. F., & Collins, R. A. 1968, Nature, 217, 709, doi: 10.1038/217709a0

Hulleman, F., van Kerkwijk, M. H., & Kulkarni, S. R. 2000, Nature, 408, 689, doi: 10.1038/35047024

—. 2004, Astronomy & Astrophysics, 416, 1037, doi: 10.1051/0004-6361:20031756

Inutsuka, S.-i., & Sano, T. 2005, The Astrophysical Journal Letters, 628, L155, doi: 10.1086/432796

Kaplan, D. L., & van Kerkwijk, M. H. 2009a, The Astrophysical Journal Letters, 692, L62, doi: 10.1088/0004-637X/692/1/L62

—. 2009b, The Astrophysical Journal, 705, 798, doi: 10.1088/0004-637X/705/1/798

—. 2011, The Astrophysical Journal Letters, 740, L30, doi: 10.1088/2041-8205/740/1/L30

Kaspi, V. M., Gavriil, F. P., Woods, P. M., et al. 2003, The Astrophysical Journal Letters, 588, L93, doi: 10.1086/375683

Keane, E. F., Kramer, M., Lyne, A. G., Stappers, B. W., & McLaughlin, M. A. 2011, Monthly Notices of the Royal Astronomical Society, 415, 3065, doi: 10.1111/j.1365-2966.2011.18917.x

Konar, S., & Bhattacharya, D. 1997, Monthly Notices of the Royal Astronomical Society, 284, 311, doi: 10.1093/mnras/284.2.311

Lamb, F. K., Pethick, C. J., & Pines, D. 1973, The Astrophysical Journal, 184, 271, doi: 10.1086/152325

Lewin, W. H. G., van Paradijs, J., & van den Heuvel, E. P. J. 1997, X-ray Binaries (Cambridge, UK: Cambridge University Press)

Manchester, R. N., Hobbs, G. B., Teoh, A., & Hobbs, M. 2005, The Astrophysical Journal, 129, 1993, doi: 10.1086/428488

Marsden, D., Lingenfelter, R. E., Rothschild, R. E., & Higdon, J. C. 2001, The Astrophysical Journal, 550, 397, doi: 10.1086/319701

McLaughlin, M. A., Lyne, A. G., Lorimer, D. R., et al. 2006, Nature, 439, 817, doi: 10.1038/nature04440

Menou, K., Perna, R., & Hernquist, L. 2001, The Astrophysical Journal Letters, 554, L63, doi: 10.1086/320927

Mereghetti, S. 2011, Astrophysics and Space Science Proceedings, 21, 345, doi: 10.1007/978-3-642-17251-9_29

—. 2013, Brazilian Journal of Physics, 43, 356, doi: 10.1007/s13538-013-0137-y

Michel, F. C. 1988, Nature, 333, 644, doi: 10.1038/333644a0

Michel, F. C., & Dessler, A. J. 1981, The Astrophysical Journal, 251, 654, doi: 10.1086/159511

Morello, V., Keane, E. F., Enoto, T., et al. 2020, Monthly Notices of the Royal Astronomical Society, 493, 1165, doi: 10.1093/mnras/staa321

Morii, M., Kawai, N., Kataoka, J., et al. 2005, Advances in Space Research, 35, 1177, doi: 10.1016/j.asr.2005.04.051

Olausen, S. A., Zhu, W. W., Vogel, J. K., et al. 2013, The Astrophysical Journal, 764, 1, doi: 10.1088/0004-637X/764/1/1

Oppenheimer, J. R., & Volkoff, G. M. 1939, Physical Review, 55, 374, doi: 10.1103/PhysRev.55.374

Page, D. 2009, in Astrophysics and Space Science Library, Vol. 357, Astrophysics and Space Science Library, ed. W. Becker, 247

Page, D., Geppert, U., & Weber, F. 2006, Nuclear Physics A, 777, 497–530, doi: 10.1016/j.nuclphysa.2005.09.019

Pavlov, G. G., Zavlin, V. E., Sanwal, D., Burwitz, V., & Garmire, G. P. 2001, The Astrophysical Journal Letters, 552, L129, doi: 10.1086/320342

Perna, R., Duffell, P., Cantiello, M., & MacFadyen, A. I. 2014, The Astrophysical Journal, 781, 119, doi: 10.1088/0004-637X/781/2/119

Perna, R., Hernquist, L., & Narayan, R. 2000, The Astrophysical Journal, 541, 344, doi: 10.1086/309404

Popov, S. B., Turolla, R., & Possenti, A. 2006, Monthly Notices of the Royal Astronomical Society, 369, L23, doi: 10.1111/j.1745-3933.2006.00166.x

Popov, S. B., Turolla, R., Prokhorov, M. E., Colpi, M., & Treves, A. 2005, Applied Surface Science, 299, 117, doi: 10.1007/s10509-005-5160-1

Potekhin, A. Y., & Chabrier, G. 2018, Astronomy & Astrophysics, 609, A74, doi: 10.1051/0004-6361/201731866

Potekhin, A. Y., Zyuzin, D. A., Yakovlev, D. G., Beznogov, M. V., & Shibanov, Y. A. 2020, Monthly Notices of the Royal Astronomical Society, doi: 10.1093/mnras/staa1871

Radhakrishnan, V., & Srinivasan, G. 1982, Current Science, 51, 1096

Rea, N., Israel, G. L., Esposito, P., et al. 2012, The Astrophysical Journal, 754, 27, doi: 10.1088/0004-637X/754/1/27

Reynolds, S. P., Borkowski, K. J., Gaensler, B. M., et al. 2006, The Astrophysical Journall, 639, L71, doi: 10.1086/502648

Rigoselli, M., Mereghetti, S., Suleimanov, V., et al. 2019, Astronomy & Astrophysics, 627, A69, doi: 10.1051/0004-6361/201935485

Shakura, N. I., & Sunyaev, R. A. 1973, Astronomy & Astrophysics, 24, 337

Shklovsky, I. S. 1967, The Astrophysical Journal Letters, 148, L1, doi: 10.1086/180001

Speagle, J. S., Kaplan, D. L., & van Kerkwijk, M. H. 2011, The Astrophysical Journal, 743, 183, doi: 10.1088/0004-637X/743/2/183

Srinivasan, G., Bhattacharya, D., Muslimov, A. G., & Tsygan, A. J. 1990, Current Science, 59, 31

Sterne, T. E. 1933, Monthly Notices of the Royal Astronomical Society, 93, 736, doi: 10.1093/mnras/93.9.736

Tan, C. M., Bassa, C. G., Cooper, S., et al. 2018, The Astrophysical Journal, 866, 54, doi: 10.3847/1538-4357/aade88

Tetzlaff, N., Eisenbeiss, T., Neuhäuser, R., & Hohle, M. M. 2011, Monthly Notices of the Royal Astronomical Society, 417, 617, doi: 10.1111/j.1365-2966.2011.19302.x

Thompson, C., & Duncan, R. C. 1995, Monthly Notices of the Royal Astronomical Society, 275, 255, doi: 10.1093/mnras/275.2.255

Tiengo, A., & Mereghetti, S. 2007, The Astrophysical Journal Letters, 657, L101, doi: 10.1086/513143

Tolman, R. C. 1939, Physical Review, 55, 364, doi: 10.1103/PhysRev.55.364

Turolla, R. 2009, Astrophysics and Space Science Library, Vol. 357, Isolated Neutron Stars: The Challenge of Simplicity (Springer Berlin Heidelberg), 141

Turolla, R., Zane, S., Pons, J. A., Esposito, P., & Rea, N. 2011, The Astrophysical Journal, 740, 105, doi: 10.1088/0004-637X/740/2/105

van den Heuvel, E. P. J., & Heise, J. 1972, Nature Physical Science, 239, 67, doi: 10. 1038/physci239067a0

Viganò, D., Rea, N., Pons, J. A., et al. 2013, Monthly Notices of the Royal Astronomical Society, 434, 123, doi: 10.1093/mnras/stt1008

Walter, F. M., Wolk, S. J., & Neuhäuser, R. 1996, Nature, 379, 233, doi: 10.1038/ 379233a0

Wang, Z., Chakrabarty, D., & Kaplan, D. L. 2006, Nature, 440, 772, doi: 10.1038/ nature04669

Watanabe, E., Shibata, S., Sakamoto, T., & Bamba, A. 2019, Monthly Notices of the Royal Astronomical Society, 486, 5323, doi: 10.1093/mnras/stz1162

White, N. E. 2002, High-mass X-ray binaries (Published by Kluwer Academic Publishers, now owned by Springer: Dordrecht), 823

Wijnands, R., & van der Klis, M. 1998, Nature, 394, 344, doi: 10.1038/28557

Yan, T., Perna, R., & Soria, R. 2012, Monthly Notices of the Royal Astronomical Society, 423, 2451, doi: 10.1111/j.1365-2966.2012.21051.x

Yao, J. M., Manchester, R. N., & Wang, N. 2017, Monthly Notices of the Royal Astronomical Society, 468, 3289, doi: 10.1093/mnras/stx729

Young, M. D., Manchester, R. N., & Johnston, S. 1999, Nature, 400, 848, doi: 10. 1038/23650